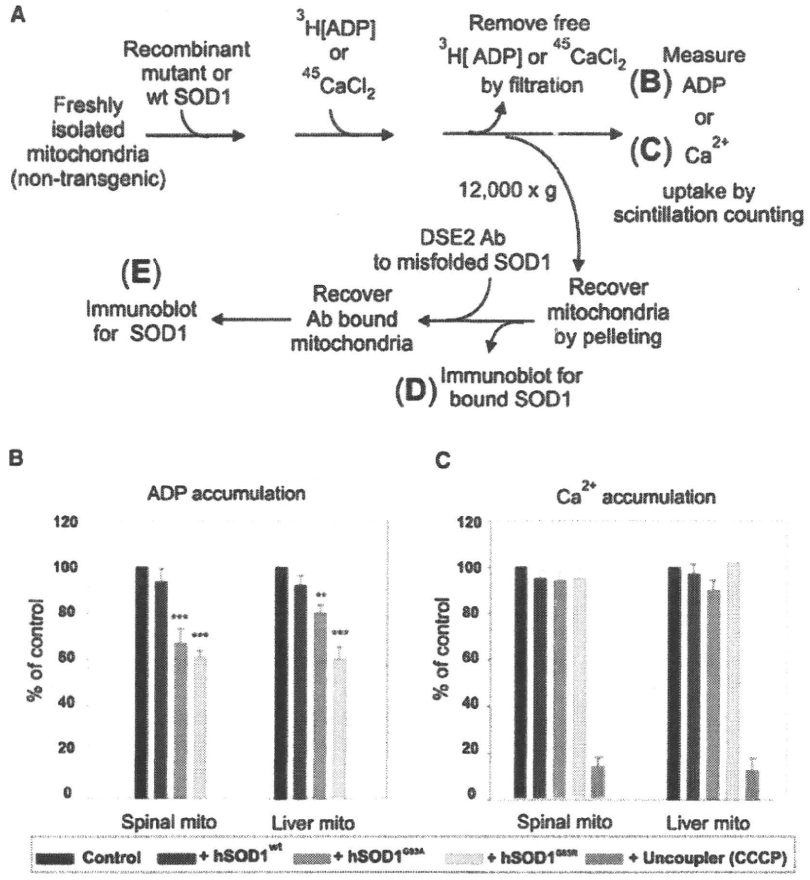


**Figure 5. Mutant SOD1 Proteins Affect ADP but Not $Ca^{2+}$ Accumulation into Mitochondria**

(A) ADP or $Ca^{2+}$ accumulation into isolated mitochondria was measured using a filter trap assay with radio-labeled $^{45}CaCl_2$ or [$^3$H]ADP. Mitochondria were isolated from fresh spinal cords and livers of nontransgenic rats.

(B) ADP and (C) $Ca^{2+}$ accumulation were measured before and after the addition of 3 μM (50 μg/ml) hSOD1$^{wt}$, hSOD1$^{G93A}$, or hSOD1$^{G85R}$ purified proteins. Student's t test was used and $p < 0.001$ (marked by three asterisks) and $p < 0.01$ (marked by two asterisks) were considered statistically significant. Values represent the means ± SEM of three independent experiments.

(D) Purified hSOD1$^{wt}$, hSOD1$^{G93A}$, or hSOD1$^{G85R}$ were incubated with liver or spinal cord mitochondrial fractions purified from a nontransgenic rat for 20 min at 37°C. The samples were then washed three times and the mitochondrial pellet was subjected to immunoblot using an SOD1 antibody.

(E) Purified hSOD1$^{wt}$, hSOD1$^{G93A}$, or hSOD1$^{G85R}$ was incubated for 20 min at 37°C with spinal cord mitochondria purified from nontransgenic rats. The samples were then washed three times and the mitochondrial pellet was subjected to immunoprecipitation using DSE2 (3H1) antibody, a monoclonal antibody only recognizing misfolded SOD1. The immunoprecipitates were immunoblotted using an SOD1 antibody.

progression to an early disease point (Figure 6B) were accelerated by 41 and 45 days, respectively, in *SOD1$^{G37R}$/VDAC1$^{+/-}$* mice (183 ± 22 and 230 ± 28 days) compared with their SOD1$^{G37R}$ littermates (224 ± 19 and 275 ± 25 days). Moreover, age at which end stage disease was reached was also reduced by an average of 59 days (Figure 6C; *SOD1$^{G37R}$/VDAC1$^{+/-}$* mice [310 ± 42 days] compared with their SOD1$^{G37R}$ littermates [369 ± 32 days]). A similar reduction in age of onset and life span was also observed for *SOD1$^{G37R}$/VDAC1$^{-/-}$* mice (Figure 4S), demonstrating that reduction in VDAC1 activity does affect SOD1 mutant-dependent pathogenesis, primarily by accelerating an early step in disease onset or spread.

## DISCUSSION

We have demonstrated here in floated spinal cord mitochondria from mutant SOD1 expressing animals that both misfolded dismutase active or inactive SOD1 mutants bind directly and selectively to the cytoplasmically exposed face of VDAC1. Both dismutase active and dismutase inactive, but not wild-type, SOD1 binding to VDAC1 reduces channel conductance, as demonstrated for $K^+$ and $Cl^-$ ions by electrophysiological recording and for ADP by inhibition of normal ADP accumulation into mitochondria. Channel conductance was not affected in liver mitochondria (where misfolded SOD1 does not accumulate). Mutant association and conductance inhibition is replicated in spinal cord mitochondria purified from mutant

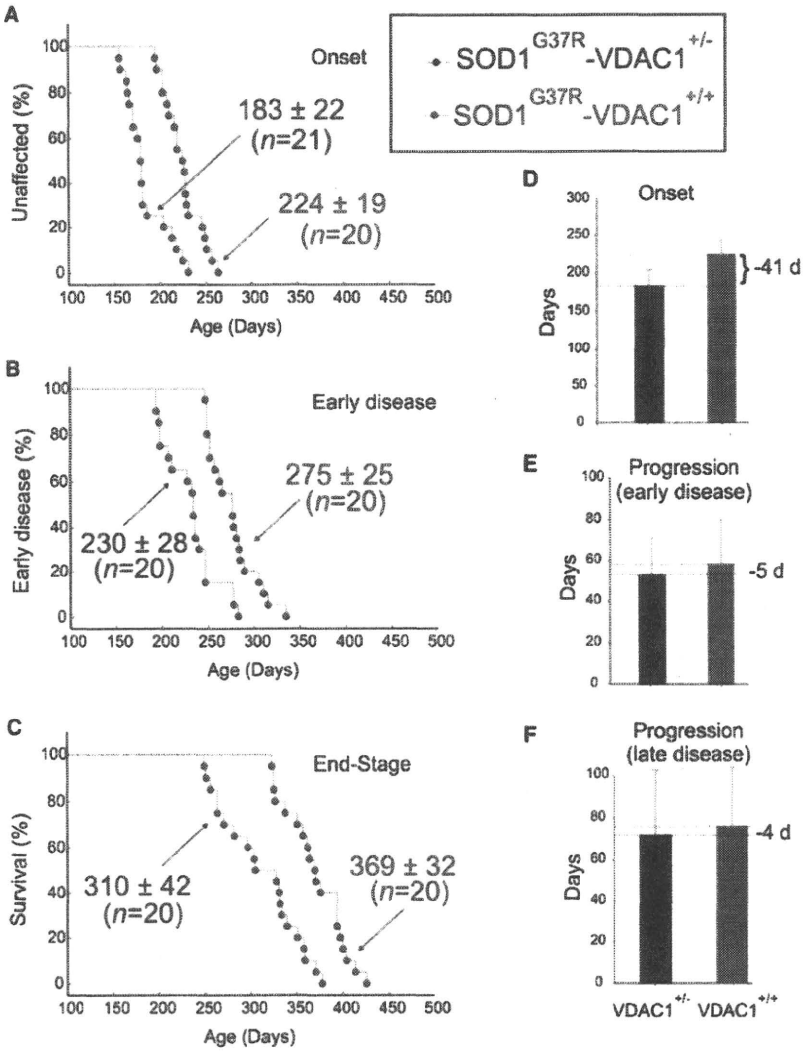


**Figure 6. Reduction of VDAC1 Levels Accelerates Disease Onset and Diminishes Survival in the hSOD1$^{G37R}$ Mouse Model of ALS**

Ages of (A) disease onset (determined as the time when mice reached peak body weight), (B) early disease (determined as the time when mice lost 10% of maximal weight), and (C) disease end stage (determined as the time when the animal could not right itself within 20 s when placed on its side) of *SOD1$^{G37R}$-VDAC1$^{+/-}$* (blue) and *SOD1$^{G37R}$-VDAC1$^{+/+}$* littermates (red). Mean ages ± SD is provided.

(D, E, and F) Mean onset (D), mean duration of early disease (from onset to 10% weight loss, E) and mean duration of late disease (from 10% weight loss to end-stage, F). Error bars denote SD. See also Figure S4.

expressing animals beginning presymptomatically and increasing in severity during disease progression contemporaneous with increased accumulation of misfolded mutant SOD1. The clear implication from this is that only the misfolded portion of SOD1 is able to affect the channel, thereby partially blocking metabolite flux across the outer mitochondrial membrane. Reduced conductance by VDAC1 will decrease ATP synthesis, increase the ADP/ATP ratio in the cytosol and reduce membrane potential (as outlined in Figure 7). Chronic mitochondrial dysfunction can in turn drive generation of damaging reactive oxygen species that could drive further SOD1 misfolding through chemical damage to it, as has been previously documented selectively in spinal cords from mutant SOD1 animals (Liu et al., 2004; Vande Velde et al., 2008). Thus, our evidence demonstrates that reduced VDAC1 conductance, and correspondingly reduced respiration rate (Lemasters and Holmuhamedov, 2006), are direct components of intracellular damage from mutant SOD1.

Moreover, not only does mutant SOD1 lower VDAC1-dependent ADP conductance by half as much as does complete VDAC1 deletion (Figure 3S), further reduction in conductance (by VDAC1 gene inactivation) significantly accelerates disease onset (but not progression), reducing survival by more than two months for both VDAC1 heterozygous and homozygous mice. Intracellular targets for SOD1 damage beyond VDAC1 have been proposed (Ilieva et al., 2009), including aberrant glutamate handling from delayed synaptic glutamate recovery by astrocytes (Rothstein et al., 1995), mutant damage in the extracellular space following aberrant cosecretion with chromogranin (Urushitani et al., 2006), endoplasmic reticulum stress from inhibition of the ERAD pathway by mutant SOD1 binding to the integral membrane protein derlin (Nishitoh et al., 2008), and excessive production by microglia of extracellular superoxide following mutant SOD1 binding to the small G protein Rac1 and its subsequent stimulation of NAPDH oxidase (Harraz et al., 2008). Moreover, it was recently proposed that misfolded SOD1 damage to mitochondria can induce morphological changes and cytochrome c release in the presence of Bcl-2 (Pedrini et al., 2010). To those hypotheses, we propose that the partial blockage of the VDAC1 channel by direct association with misfolded SOD1 would make motor neurons more vulnerable to any of these additional stresses derived either from mutant SOD1 acting within motor neurons, astrocytes, microglia, and possibly additional neighboring nonneuronal cells. Indeed, in the presence of reduced VDAC1 conductance such pathways must play roles in pathogenesis, as we have shown that mutant SOD1-mediated disease still ensues in VDAC1 null mice.

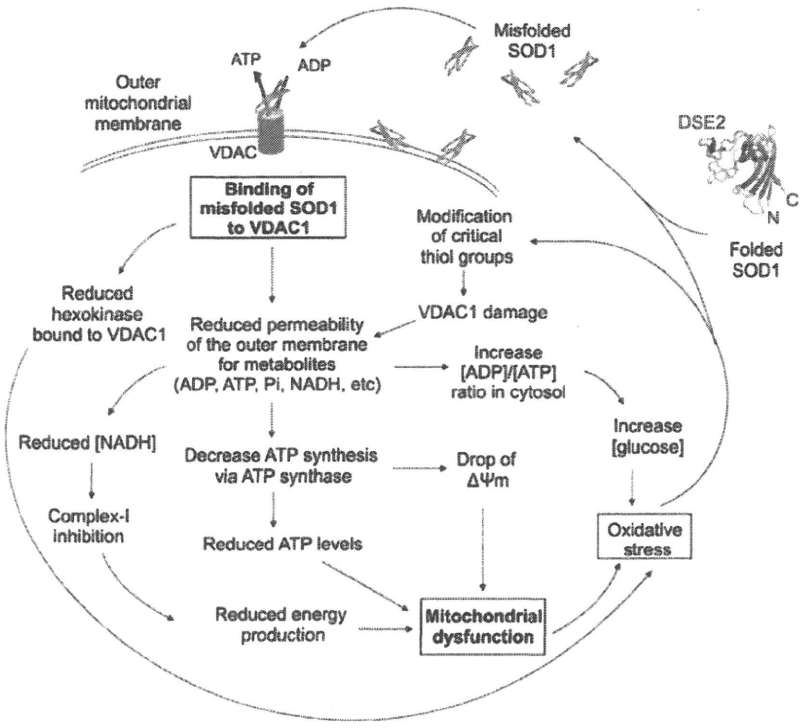


**Figure 7. Effects of Misfolded SOD1 Binding to VDAC1**

Model showing the effects of misfolded SOD1 binding to VDAC1. Misfolded SOD1 is proposed to inhibit VDAC1 conductance and suppress both uptake and release of mitochondrial metabolites.

This reduction in metabolites flux would result in reduced energy production and oxidative stress leading to mitochondrial dysfunction.

Surprisingly, in the absence of VDAC1, we have found a 60% residual ADP conductance which seems most likely to be contributed by compensatory VDACs or VDAC-like activity(ies). Although no other VDAC isoform is known to be overexpressed in VDAC1 null mice, VDAC2 has been shown to exist in two forms that differ in conductance and selectivity (Xu et al., 1999). It is plausible that in the absence of VDAC1, VDAC2 exists predominantly in a high conductance state, as a compensatory mechanism. This mechanism should now be tested by purifying VDAC2 from VDAC1 knockout mouse, and testing its channel properties in lipid bilayers.

The compromise in mutant SOD1-mediated VDAC1 conductance that we have found offers a mechanistic explanation for alteration in mitochondrial electron transfer chain complexes and the capacity to consume oxygen and synthesize ATP previously reported in one mutant SOD1 expressing mouse line (Jung et al., 2002; Kirkinezos et al., 2005; Mattiazzi et al., 2002). The recent report that association of $hSOD1^{G93A}$ and $hSOD1^{G85R}$ with motor neuron mitochondria reduces capacity of the electron transfer chain to limit $Ca^{2+}$-induced $\Psi m$ depolarization (Nguyen et al., 2009) is also fully compatible with altered adenine nucleotide transport across the outer mitochondrial membrane as the initiating deficit. So too is the report of reduced ability of mitochondria from $SOD1^{G93A}$ and $SOD1^{G85R}$ mice to survive repetitive $Ca^{2+}$ addition (Damiano et al., 2006).

VDAC1 has been proposed to be the mediator for ROS release from the intermitochondrial spaces to the cytosol (Han et al., 2003; Madesh and Hajnóczky, 2001). Moreover, hexokinase (known to interact with VDAC1) has been shown in cell culture to decrease ROS release when overexpressed, thereby reducing intracellular levels of ROS (Ahmad et al., 2002; da-Silva et al., 2004). The relatively low level of hexokinase in spinal cord as compared to that in brain (Figure 1F) may therefore be a component of selective vulnerability. This is also consistent with the selective association of misfolded mutant SOD1 with VDAC1 on the cytoplasmic face of mitochondria from spinal cord, but not liver or brain. Although both tissues accumulate high levels of mutant SOD1 (Liu et al., 2004; Vande Velde et al., 2008), prior findings show that misfolded mutant SOD1 is bound to the cytoplasmic face of spinal cord mitochondria, while apparently imported into the intermembrane space of mitochondria from cortex of the same animals and not associated with liver mitochondria at all (Vande Velde et al., 2008). Another factor likely underlying the differences in mutant SOD1 association with mitochondria, and therefore potentially factors underlying selective vulnerability, is that mitochondria from different tissues (and which retain different functional properties) have different protein compositions (Bailey et al., 2007; Mootha et al., 2003), including hexokinase levels. This is accompanied by intrinsic differences in $O_2^{-\cdot}$ production, lipid peroxidation, DNA oxidation and $Ca^{2+}$ accumulation capacity (Sullivan et al., 2004).

Our finding that VDAC1 is one of the targets for misfolded SOD1 within the nervous system raises substantial implications for the mechanism underlying premature degeneration and death of motor neurons. A variety of apoptotic stimuli are known to trigger cell death by modulation of VDAC1 (Abu-Hamad et al., 2008; Shoshan-Barmatz et al., 2006; Tsujimoto and Shimizu, 2002; Yagoda et al., 2007; Zaid et al., 2005; Zamzami and Kroemer, 2003; Zheng et al., 2004), implicating VDAC1 as a component of the apoptotic machinery. Although VDAC1 proteins have been reported to be dispensable for $Ca^{2+}$ and oxidative stress-induced permeability transition pore (PTP) opening (Baines et al., 2007), siRNA-mediated reduction in VDAC1 has supported VDAC1 as an indispensable protein for endostatin-, cisplatin-, and selenite-induced oxidative stress induced PTP opening and apoptosis (Tajeddine et al., 2008; Tomasello et al., 2009; Yuan et al., 2008). Moreover, VDAC1 was recently shown to be involved in staurosporine- and

ceramide-induced cell death downstream of BAD and BCL-$X_L$ (Roy et al., 2009) and curcumin induced apoptosis by cooperating with Bax in the release of AIF from mitochondria (Scharstuhl et al., 2009). Since VDAC1 is one of several targets for a cholesterol-like small molecule (TRO19622) that can protect motor neurons from SOD1 mutant-mediated death in culture and modestly delay disease onset in SOD1 mutant mice (Bordet et al., 2007), it now seems likely that its efficacy may be through direct effect on VDAC1.

Finally, it is well established that although motor neurons are the final targets in ALS, mutant damage within astrocytes and microglia contributes to driving rapid disease progression (Beers et al., 2006; Boillée et al., 2006a, 2006b; Clement et al., 2003; Yamanaka et al., 2008a, 2008b). In this context, we show here that little accumulation of misfolded SOD1 is found by disease onset, but it is preferentially within motor neurons. However, during disease progression a dramatic increase of misfolded SOD1 is observed accumulated in other cells as well and probably extracellularly. Interestingly, mitochondrial dysfunction(s) within mutant astrocytes has been reported to cause acute motor neuron death in astrocyte-motor neuron cocultures (Cassina et al., 2008) and astrocytes expressing mutant SOD1 have been reported to induce mitochondrial dysfunction within motor neurons (Bilsland et al., 2008). Coupling these findings with the appearance of aberrant mitochondria within motor neurons in multiple animal models of SOD1 mutant mediated ALS (Bendotti et al., 2001; Jaarsma et al., 2001; Kong and Xu, 1998; Wong et al., 1995) and the association of mutant SOD1 with mitochondria within affected tissues, we propose that misfolded SOD1 association directly with VDAC1 represents a primary event of damage within motor neurons.

## EXPERIMENTAL PROCEDURES

### Transgenic Rats and Mice

Transgenic rats expressing $hSOD1^{wt}$ (Chan et al., 1998), $hSOD1^{G93A}$ (Howland et al., 2002), and $hSOD1^{H46R}$ (Nagai et al., 2001) were as originally described. All animal procedures were consistent with the requirements of the Animal Care and Use Committee of the University of California.

Mice heterozygous for the mutant human $SOD1^{G37R}$ transgene ($LoxSOD1^{G37R}$) (Boillée et al., 2006b) were crossed with mice heterozygous for a VDAC1 gene disruption (Weeber et al., 2002). Mice were genotyped by PCR for the presence of the mutant SOD1 transgene (Williamson and Cleveland, 1999) and using a four-primer multiplex PCR for the presence of VDAC1 (Weeber et al., 2002), as previously described.

For survival experiments, $SOD1^{G37R}$, $VDAC1^{+/-}$ mice were always compared with their contemporaneously produced $SOD1^{G37R}$, $VDAC1^{+/+}$ littermates. Time of disease onset was retrospectively determined as the time when mice reached peak body weight, early disease was defined at the time when denervation-induced muscle atrophy had produced a 10% loss of maximal weight, and end-stage was determined by paralysis so severe that the animal could not right itself within 20 s when placed on its side, an endpoint frequently used for SOD1 mutant mice and one that was consistent with the requirements of the Animal Care and Use Committee of the University of California.

### Subcellular Fractionation

Mitochondria were purified as previously described (Vande Velde et al., 2008). Tissues were homogenized on ice in 5 volumes of ice-cold homogenization buffer (HB) composed of 210 mM mannitol, 70 mM sucrose, 1 mM EDTA-(Tris) and 10 mM Tris-HCl (pH 7.2). Homogenates were centrifuged at 1,000 × g for 10 min. Supernatants were recovered, and pellets were washed with ½ volume HB and centrifuged at 1,000 × g. Supernatants were pooled and centrifuged at 12,000 × g for 15 min to yield a crude mitochondrial pellet. The supernatant was used to make cytosolic fractions by further centrifugation at 100,000 × g for 1 hr. The mitochondria were gently resuspended in HB and then adjusted to 1.204 g/ml Optiprep (iodixanol) and loaded on the bottom of a polycarbonate tube. Mitochondria were overlaid with an equal volume of 1.175 g/ml and 1.079 g/ml Optiprep and centrifuged at 50,000 × g for 4 hr (SW-55; Beckman). Mitochondria were collected at the 1.079/1.175 g/ml interface and washed once to remove the Optiprep. Optiprep stock solution was diluted in 250 mM sucrose, 120 mM Tris-HCl (pH 7.4), 6 mM EDTA plus protease inhibitors.

For activity assays, spinal cords were homogenized in 5 volumes of ice-cold homogenization buffer (HB) on ice. Homogenates were centrifuged at 1,000 × g for 5 min. Supernatants were recovered and centrifuged again at 1,000 × g for 5 min. Supernatants were centrifuged at 12,000 × g for 10 min to yield crude mitochondrial pellets. These mitochondria were gently resuspended in HB and then adjusted to 12% Optiprep (iodixanol) and centrifuged at 17,000 × g for 10 min (SW-55; Beckman). The majority of the myelin (at the top of the sample) was removed and the mitochondria were washed once with HB (without EDTA) to remove the Optiprep.

Liver was homogenized in 5 volumes of ice-cold homogenization buffer (HB) on ice. Homogenates were centrifuged at 1,000 × g for 5 min. Supernatants were recovered, and centrifuged again at 1,000 × g for 5 min. Supernatant was centrifuged at 12,000 × g for 10 min to yield a crude mitochondrial pellet. These mitochondria were resuspended in HB (without EDTA) and centrifuged again at 12,000 × g for 10 min. The pellet was resuspended in a small volume of HB without EDTA.

### VDAC Channel Recording and Analysis

Reconstitution of VDAC into a planar lipid bilayer (PLB), single channel current recording, and data analysis were carried out as previously described (Gincel et al., 2001). Briefly, PLB were prepared from soybean asolectin dissolved in n-decane (50 mg/ml). Only PLB with a resistance greater than 100 GΩ, were used. Purified protein (about 1 ng) was added to the *cis* chamber. After one or a few channels were inserted into the PLB, the excess protein was removed by perfusion of the *cis* chamber with 20 volumes of a solution to prevent further incorporation. Currents were recorded under voltage-clamp using a Bilayer Clamp BC-525B amplifier (Warner Instrument Corp.). The currents were measured with respect to the *trans* side of the membrane (ground). The currents were low-pass, filtered at 1 kHz and digitized online using a Digidata 1200 interface board and pCLAMP 6 software (Axon Instruments, Inc.). Sigma Plot 6.0 scientific software (Jandel Scientific) was used for curve fitting. All experiments were performed at room temperature.

Please see Supplemental Information for the following experimental procedures: Protein Purification, Immunoprecipitation, DSE2 antibodies, Immunostaining, $Ca^{2+}$ and ADP Accumulation by Mitochondria, and Immunoblotting.

## SUPPLEMENTAL INFORMATION

Supplemental Information includes four figures and Supplemental Experimental Procedures and can be found with this article online at doi:10.1016/j.neuron.2010.07.019.

## ACKNOWLEDGMENTS

We would like to thank Neil Cashman (University of British Columbia) and Amorfix Life Sciences (Vancouver) for generously providing us with DSE2 antibodies, William Craigen (Baylor College of Medicine) for VDAC1 knockout mice, and Larry Hayward (UMass Medical School) for wild type and mutant SOD1 baculovirus stock. This work has been supported by a grant from the NIH (R37 NS27036). A.I. has been supported by EMBO Long-Term Fellowship and by a postdoctoral fellowship from IsrALS. D.W.C. receives salary support from the Ludwig Institute for Cancer Research.

Accepted: July 22, 2010
Published: August 25, 2010

**REFERENCES**

Abu-Hamad, S., Sivan, S., and Shoshan-Barmatz, V. (2006). The expression level of the voltage-dependent anion channel controls life and death of the cell. Proc. Natl. Acad. Sci. USA *103*, 5787–5792.

Abu-Hamad, S., Zaid, H., Israelson, A., Nahon, E., and Shoshan-Barmatz, V. (2008). Hexokinase-I protection against apoptotic cell death is mediated via interaction with the voltage-dependent anion channel-1: mapping the site of binding. J. Biol. Chem. *283*, 13482–13490.

Abu-Hamad, S., Arbel, N., Calo, D., Arzoine, L., Israelson, A., Keinan, N., Ben-Romano, R., Friedman, O., and Shoshan-Barmatz, V. (2009). The VDAC1 N-terminus is essential both for apoptosis and the protective effect of anti-apoptotic proteins. J. Cell Sci. *122*, 1906–1916.

Ahmad, A., Ahmad, S., Schneider, B.K., Allen, C.B., Chang, L.Y., and White, C.W. (2002). Elevated expression of hexokinase II protects human lung epithelial-like A549 cells against oxidative injury. Am. J. Physiol. *283*, L573–L584.

Arbel, N., and Shoshan-Barmatz, V. (2010). Voltage-dependent anion channel 1-based peptides interact with Bcl-2 to prevent antiapoptotic activity. J. Biol. Chem. *285*, 6053–6062.

Azoulay-Zohar, H., Israelson, A., Abu-Hamad, S., and Shoshan-Barmatz, V. (2004). In self-defence: hexokinase promotes voltage-dependent anion channel closure and prevents mitochondria-mediated apoptotic cell death. Biochem. J. *377*, 347–355.

Bailey, A.O., Miller, T.M., Dong, M.Q., Vande Velde, C., Cleveland, D.W., and Yates, J.R. (2007). RCADiA: simple automation platform for comparative multidimensional protein identification technology. Anal. Chem. *79*, 6410–6418.

Baines, C.P., Kaiser, R.A., Sheiko, T., Craigen, W.J., and Molkentin, J.D. (2007). Voltage-dependent anion channels are dispensable for mitochondrial-dependent cell death. Nat. Cell Biol. *9*, 550–555.

Beers, D.R., Henkel, J.S., Xiao, Q., Zhao, W., Wang, J., Yen, A.A., Siklos, L., McKercher, S.R., and Appel, S.H. (2006). Wild-type microglia extend survival in PU.1 knockout mice with familial amyotrophic lateral sclerosis. Proc. Natl. Acad. Sci. USA *103*, 16021–16026.

Bendotti, C., Calvaresi, N., Chiveri, L., Prelle, A., Moggio, M., Braga, M., Silani, V., and De Biasi, S. (2001). Early vacuolization and mitochondrial damage in motor neurons of FALS mice are not associated with apoptosis or with changes in cytochrome oxidase histochemical reactivity. J. Neurol. Sci. *191*, 25–33.

Benz, R. (1994). Permeation of hydrophilic solutes through mitochondrial outer membranes: review on mitochondrial porins. Biochim. Biophys. Acta *1197*, 167–196.

Bergemalm, D., Jonsson, P.A., Graffmo, K.S., Andersen, P.M., Brännström, T., Rehnmark, A., and Marklund, S.L. (2006). Overloading of stable and exclusion of unstable human superoxide dismutase-1 variants in mitochondria of murine amyotrophic lateral sclerosis models. J. Neurosci. *26*, 4147–4154.

Bilsland, L.G., Nirmalananthan, N., Yip, J., Greensmith, L., and Duchen, M.R. (2008). Expression of mutant SOD1 in astrocytes induces functional deficits in motoneuron mitochondria. J. Neurochem. *107*, 1271–1283.

Boillée, S., Vande Velde, C., and Cleveland, D.W. (2006a). ALS: a disease of motor neurons and their nonneuronal neighbors. Neuron *52*, 39–59.

Boillée, S., Yamanaka, K., Lobsiger, C.S., Copeland, N.G., Jenkins, N.A., Kassiotis, G., Kollias, G., and Cleveland, D.W. (2006b). Onset and progression in inherited ALS determined by motor neurons and microglia. Science *312*, 1389–1392.

Bordet, T., Buisson, B., Michaud, M., Drouot, C., Galéa, P., Delaage, P., Akentieva, N.P., Evers, A.S., Covey, D.F., Ostuni, M.A., et al. (2007). Identification and characterization of cholest-4-en-3-one, oxime (TRO19622), a novel drug candidate for amyotrophic lateral sclerosis. J. Pharmacol. Exp. Ther. *322*, 709–720.

Bruijn, L.I., Becher, M.W., Lee, M.K., Anderson, K.L., Jenkins, N.A., Copeland, N.G., Sisodia, S.S., Rothstein, J.D., Borchelt, D.R., Price, D.L., and Cleveland, D.W. (1997). ALS-linked SOD1 mutant G85R mediates damage to astrocytes and promotes rapidly progressive disease with SOD1-containing inclusions. Neuron *18*, 327–338.

Cashman, N.R., and Caughey, B. (2004). Prion diseases—close to effective therapy? Nat. Rev. Drug Discov. *3*, 874–884.

Cassina, P., Cassina, A., Pehar, M., Castellanos, R., Gandelman, M., de León, A., Robinson, K.M., Mason, R.P., Beckman, J.S., Barbeito, L., and Radi, R. (2008). Mitochondrial dysfunction in SOD1G93A-bearing astrocytes promotes motor neuron degeneration: prevention by mitochondrial-targeted antioxidants. J. Neurosci. *28*, 4115–4122.

Chan, P.H., Kawase, M., Murakami, K., Chen, S.F., Li, Y., Calagui, B., Reola, L., Carlson, E., and Epstein, C.J. (1998). Overexpression of SOD1 in transgenic rats protects vulnerable neurons against ischemic damage after global cerebral ischemia and reperfusion. J. Neurosci. *18*, 8292–8299.

Clement, A.M., Nguyen, M.D., Roberts, E.A., Garcia, M.L., Boillée, S., Rule, M., McMahon, A.P., Doucette, W., Siwek, D., Ferrante, R.J., et al. (2003). Wild-type nonneuronal cells extend survival of SOD1 mutant motor neurons in ALS mice. Science *302*, 113–117.

Cleveland, D.W., and Rothstein, J.D. (2001). From Charcot to Lou Gehrig: deciphering selective motor neuron death in ALS. Nat. Rev. Neurosci. *2*, 806–819.

Colombini, M. (2004). VDAC: the channel at the interface between mitochondria and the cytosol. Mol. Cell. Biochem. *256-257*, 107–115.

da-Silva, W.S., Gómez-Puyou, A., de Gómez-Puyou, M.T., Moreno-Sanchez, R., De Felice, F.G., de Meis, L., Oliveira, M.F., and Galina, A. (2004). Mitochondrial bound hexokinase activity as a preventive antioxidant defense: steady-state ADP formation as a regulatory mechanism of membrane potential and reactive oxygen species generation in mitochondria. J. Biol. Chem. *279*, 39846–39855.

Dal Canto, M.C., and Gurney, M.E. (1994). Development of central nervous system pathology in a murine transgenic model of human amyotrophic lateral sclerosis. Am. J. Pathol. *145*, 1271–1279.

Damiano, M., Starkov, A.A., Petri, S., Kipiani, K., Kiaei, M., Mattiazzi, M., Flint Beal, M., and Manfredi, G. (2006). Neural mitochondrial Ca2+ capacity impairment precedes the onset of motor symptoms in G93A Cu/Zn-superoxide dismutase mutant mice. J. Neurochem. *96*, 1349–1361.

Deng, H.X., Shi, Y., Furukawa, Y., Zhai, H., Fu, R., Liu, E., Gorrie, G.H., Khan, M.S., Hung, W.Y., Bigio, E.H., et al. (2006). Conversion to the amyotrophic lateral sclerosis phenotype is associated with intermolecular linked insoluble aggregates of SOD1 in mitochondria. Proc. Natl. Acad. Sci. USA *103*, 7142–7147.

Dupuis, L., di Scala, F., Rene, F., de Tapia, M., Oudart, H., Pradat, P.F., Meininger, V., and Loeffler, J.P. (2003). Up-regulation of mitochondrial uncoupling protein 3 reveals an early muscular metabolic defect in amyotrophic lateral sclerosis. FASEB J. *17*, 2091–2093.

Echaniz-Laguna, A., Zoll, J., Ribera, F., Tranchant, C., Warter, J.M., Lonsdorfer, J., and Lampert, E. (2002). Mitochondrial respiratory chain function in skeletal muscle of ALS patients. Ann. Neurol. *52*, 623–627.

Geisler, S., Holmström, K.M., Skujat, D., Fiesel, F.C., Rothfuss, O.C., Kahle, P.J., and Springer, W. (2010). PINK1/Parkin-mediated mitophagy is dependent on VDAC1 and p62/SQSTM1. Nat. Cell Biol. *12*, 119–131.

Gincel, D., Zaid, H., and Shoshan-Barmatz, V. (2001). Calcium binding and translocation by the voltage-dependent anion channel: a possible regulatory mechanism in mitochondrial function. Biochem. J. *358*, 147–155.

Han, D., Antunes, F., Canali, R., Rettori, D., and Cadenas, E. (2003). Voltage-dependent anion channels control the release of the superoxide anion from mitochondria to cytosol. J. Biol. Chem. *278*, 5557–5563.

Harraz, M.M., Marden, J.J., Zhou, W., Zhang, Y., Williams, A., Sharov, V.S., Nelson, K., Luo, M., Paulson, H., Schöneich, C., and Engelhardt, J.F. (2008). SOD1 mutations disrupt redox-sensitive Rac regulation of NADPH oxidase in a familial ALS model. J. Clin. Invest. *118*, 659–670.

Hayward, L.J., Rodriguez, J.A., Kim, J.W., Tiwari, A., Goto, J.J., Cabelli, D.E., Valentine, J.S., and Brown, R.H., Jr. (2002). Decreased metallation and activity in subsets of mutant superoxide dismutases associated with familial amyotrophic lateral sclerosis. J. Biol. Chem. *277*, 15923–15931.

Higgins, C.M., Jung, C., and Xu, Z. (2003). ALS-associated mutant SOD1G93A causes mitochondrial vacuolation by expansion of the intermembrane space

and by involvement of SOD1 aggregation and peroxisomes. BMC Neurosci. *4*, 16.

Hirano, A., Donnenfeld, H., Sasaki, S., and Nakano, I. (1984a). Fine structural observations of neurofilamentous changes in amyotrophic lateral sclerosis. J. Neuropathol. Exp. Neurol. *43*, 461–470.

Hirano, A., Nakano, I., Kurland, L.T., Mulder, D.W., Holley, P.W., and Saccomanno, G. (1984b). Fine structural study of neurofibrillary changes in a family with amyotrophic lateral sclerosis. J. Neuropathol. Exp. Neurol. *43*, 471–480.

Hodge, T., and Colombini, M. (1997). Regulation of metabolite flux through voltage-gating of VDAC channels. J. Membr. Biol. *157*, 271–279.

Howland, D.S., Liu, J., She, Y., Goad, B., Maragakis, N.J., Kim, B., Erickson, J., Kulik, J., DeVito, L., Psaltis, G., et al. (2002). Focal loss of the glutamate transporter EAAT2 in a transgenic rat model of SOD1 mutant-mediated amyotrophic lateral sclerosis (ALS). Proc. Natl. Acad. Sci. USA *99*, 1604–1609.

Ilieva, H., Polymenidou, M., and Cleveland, D.W. (2009). Non-cell autonomous toxicity in neurodegenerative disorders: ALS and beyond. J. Cell Biol. *187*, 761–772.

Israelson, A., Arzoine, L., Abu-hamad, S., Khodorkovsky, V., and Shoshan-Barmatz, V. (2005). A photoactivable probe for calcium binding proteins. Chem. Biol. *12*, 1169–1178.

Jaarsma, D., Rognoni, F., van Duijn, W., Verspaget, H.W., Haasdijk, E.D., and Holstege, J.C. (2001). CuZn superoxide dismutase (SOD1) accumulates in vacuolated mitochondria in transgenic mice expressing amyotrophic lateral sclerosis-linked SOD1 mutations. Acta Neuropathol. *102*, 293–305.

Jung, C., Higgins, C.M., and Xu, Z. (2002). Mitochondrial electron transport chain complex dysfunction in a transgenic mouse model for amyotrophic lateral sclerosis. J. Neurochem. *83*, 535–545.

Kirkinezos, I.G., Bacman, S.R., Hernandez, D., Oca-Cossio, J., Arias, L.J., Perez-Pinzon, M.A., Bradley, W.G., and Moraes, C.T. (2005). Cytochrome c association with the inner mitochondrial membrane is impaired in the CNS of G93A-SOD1 mice. J. Neurosci. *25*, 164–172.

Kong, J., and Xu, Z. (1998). Massive mitochondrial degeneration in motor neurons triggers the onset of amyotrophic lateral sclerosis in mice expressing a mutant SOD1. J. Neurosci. *18*, 3241–3250.

Lemasters, J.J., and Holmuhamedov, E. (2006). Voltage-dependent anion channel (VDAC) as mitochondrial governator—thinking outside the box. Biochim. Biophys. Acta *1762*, 181–190.

Liu, J., Lillo, C., Jonsson, P.A., Vande Velde, C., Ward, C.M., Miller, T.M., Subramaniam, J.R., Rothstein, J.D., Marklund, S., Andersen, P.M., et al. (2004). Toxicity of familial ALS-linked SOD1 mutants from selective recruitment to spinal mitochondria. Neuron *43*, 5–17.

Madesh, M., and Hajnóczky, G. (2001). VDAC-dependent permeabilization of the outer mitochondrial membrane by superoxide induces rapid and massive cytochrome c release. J. Cell Biol. *155*, 1003–1015.

Mattiazzi, M., D'Aurelio, M., Gajewski, C.D., Martushova, K., Kiaei, M., Beal, M.F., and Manfredi, G. (2002). Mutated human SOD1 causes dysfunction of oxidative phosphorylation in mitochondria of transgenic mice. J. Biol. Chem. *277*, 29626–29633.

Mootha, V.K., Bunkenborg, J., Olsen, J.V., Hjerrild, M., Wisniewski, J.R., Stahl, E., Bolouri, M.S., Ray, H.N., Sihag, S., Kamal, M., et al. (2003). Integrated analysis of protein composition, tissue diversity, and gene regulation in mouse mitochondria. Cell *115*, 629–640.

Mulder, D.W., Kurland, L.T., Offord, K.P., and Beard, C.M. (1986). Familial adult motor neuron disease: amyotrophic lateral sclerosis. Neurology *36*, 511–517.

Nagai, M., Aoki, M., Miyoshi, I., Kato, M., Pasinelli, P., Kasai, N., Brown, R.H., Jr., and Itoyama, Y. (2001). Rats expressing human cytosolic copper-zinc superoxide dismutase transgenes with amyotrophic lateral sclerosis: associated mutations develop motor neuron disease. J. Neurosci. *21*, 9246–9254.

Nguyen, K.T., García-Chacón, L.E., Barrett, J.N., Barrett, E.F., and David, G. (2009). The Psi(m) depolarization that accompanies mitochondrial Ca2+ uptake is greater in mutant SOD1 than in wild-type mouse motor terminals. Proc. Natl. Acad. Sci. USA *106*, 2007–2011.

Nishitoh, H., Kadowaki, H., Nagai, A., Maruyama, T., Yokota, T., Fukutomi, H., Noguchi, T., Matsuzawa, A., Takeda, K., and Ichijo, H. (2008). ALS-linked mutant SOD1 induces ER stress- and ASK1-dependent motor neuron death by targeting Derlin-1. Genes Dev. *22*, 1451–1464.

Paramithiotis, E., Pinard, M., Lawton, T., LaBoissiere, S., Leathers, V.L., Zou, W.Q., Estey, L.A., Lamontagne, J., Lehto, M.T., Kondejewski, L.H., et al. (2003). A prion protein epitope selective for the pathologically misfolded conformation. Nat. Med. *9*, 893–899.

Pedrini, S., Sau, D., Guareschi, S., Bogush, M., Brown, R.H., Jr., Naniche, N., Kia, A., Trotti, D., and Pasinelli, P. (2010). ALS-linked mutant SOD1 damages mitochondria by promoting conformational changes in Bcl-2. Hum. Mol. Genet. *19*, 2974–2986.

Rakhit, R., Robertson, J., Vande Velde, C., Horne, P., Ruth, D.M., Griffin, J., Cleveland, D.W., Cashman, N.R., and Chakrabartty, A. (2007). An immunological epitope selective for pathological monomer-misfolded SOD1 in ALS. Nat. Med. *13*, 754–759.

Rosen, D.R., Siddique, T., Patterson, D., Figlewicz, D.A., Sapp, P., Hentati, A., Donaldson, D., Goto, J., O'Regan, J.P., Deng, H.X., et al. (1993). Mutations in Cu/Zn superoxide dismutase gene are associated with familial amyotrophic lateral sclerosis. Nature *362*, 59–62.

Rostovtseva, T.K., and Bezrukov, S.M. (1998). ATP transport through a single mitochondrial channel, VDAC, studied by current fluctuation analysis. Biophys. J. *74*, 2365–2373.

Rostovtseva, T., and Colombini, M. (1997). VDAC channels mediate and gate the flow of ATP: implications for the regulation of mitochondrial function. Biophys. J. *72*, 1954–1962.

Rothstein, J.D., Van Kammen, M., Levey, A.I., Martin, L.J., and Kuncl, R.W. (1995). Selective loss of glial glutamate transporter GLT-1 in amyotrophic lateral sclerosis. Ann. Neurol. *38*, 73–84.

Roy, S.S., Madesh, M., Davies, E., Antonsson, B., Danial, N., and Hajnóczky, G. (2009). Bad targets the permeability transition pore independent of Bax or Bak to switch between $Ca^{2+}$-dependent cell survival and death. Mol. Cell *33*, 377–388.

Sasaki, S., and Iwata, M. (1996). Dendritic synapses of anterior horn neurons in amyotrophic lateral sclerosis: an ultrastructural study. Acta Neuropathol. *91*, 278–283.

Sasaki, S., and Iwata, M. (2007). Mitochondrial alterations in the spinal cord of patients with sporadic amyotrophic lateral sclerosis. J. Neuropathol. Exp. Neurol. *66*, 10–16.

Scharstuhl, A., Mutsaers, H.A., Pennings, S.W., Russel, F.G., and Wagener, F.A. (2009). Involvement of VDAC, Bax and ceramides in the efflux of AIF from mitochondria during curcumin-induced apoptosis. PLoS ONE *4*, e6688. 10.1371/journal.pone.0006688.

Shimizu, S., Narita, M., and Tsujimoto, Y. (1999). Bcl-2 family proteins regulate the release of apoptogenic cytochrome c by the mitochondrial channel VDAC. Nature *399*, 483–487.

Shoshan-Barmatz, V., Israelson, A., Brdiczka, D., and Sheu, S.S. (2006). The voltage-dependent anion channel (VDAC): function in intracellular signalling, cell life and cell death. Curr. Pharm. Des. *12*, 2249–2270.

Shoshan-Barmatz, V., Keinan, N., and Zaid, H. (2008). Uncovering the role of VDAC in the regulation of cell life and death. J. Bioenerg. Biomembr. *40*, 183–191.

Sullivan, P.G., Rabchevsky, A.G., Keller, J.N., Lovell, M., Sodhi, A., Hart, R.P., and Scheff, S.W. (2004). Intrinsic differences in brain and spinal cord mitochondria: Implication for therapeutic interventions. J. Comp. Neurol. *474*, 524–534.

Tajeddine, N., Galluzzi, L., Kepp, O., Hangen, E., Morselli, E., Senovilla, L., Araujo, N., Pinna, G., Larochette, N., Zamzami, N., et al. (2008). Hierarchical involvement of Bak, VDAC1 and Bax in cisplatin-induced cell death. Oncogene *27*, 4221–4232.

Tomasello, F., Messina, A., Lartigue, L., Schembri, L., Medina, C., Reina, S., Thoraval, D., Crouzet, M., Ichas, F., De Pinto, V., and De Giorgi, F. (2009). Outer membrane VDAC1 controls permeability transition of the inner mitochondrial

membrane in cellulo during stress-induced apoptosis. Cell Res. *19*, 1363–1376.

Tsujimoto, Y., and Shimizu, S. (2002). The voltage-dependent anion channel: an essential player in apoptosis. Biochimie *84*, 187–193.

Urushitani, M., Sik, A., Sakurai, T., Nukina, N., Takahashi, R., and Julien, J.P. (2006). Chromogranin-mediated secretion of mutant superoxide dismutase proteins linked to amyotrophic lateral sclerosis. Nat. Neurosci. *9*, 108–118.

Urushitani, M., Ezzi, S.A., and Julien, J.P. (2007). Therapeutic effects of immunization with mutant superoxide dismutase in mice models of amyotrophic lateral sclerosis. Proc. Natl. Acad. Sci. USA *104*, 2495–2500.

Vande Velde, C., Miller, T.M., Cashman, N.R., and Cleveland, D.W. (2008). Selective association of misfolded ALS-linked mutant SOD1 with the cytoplasmic face of mitochondria. Proc. Natl. Acad. Sci. USA *105*, 4022–4027.

Vielhaber, S., Winkler, K., Kirches, E., Kunz, D., Büchner, M., Feistner, H., Elger, C.E., Ludolph, A.C., Riepe, M.W., and Kunz, W.S. (1999). Visualization of defective mitochondrial function in skeletal muscle fibers of patients with sporadic amyotrophic lateral sclerosis. J. Neurol. Sci. *169*, 133–139.

Vijayvergiya, C., Beal, M.F., Buck, J., and Manfredi, G. (2005). Mutant superoxide dismutase 1 forms aggregates in the brain mitochondrial matrix of amyotrophic lateral sclerosis mice. J. Neurosci. *25*, 2463–2470.

Weeber, E.J., Levy, M., Sampson, M.J., Anflous, K., Armstrong, D.L., Brown, S.E., Sweatt, J.D., and Craigen, W.J. (2002). The role of mitochondrial porins and the permeability transition pore in learning and synaptic plasticity. J. Biol. Chem. *277*, 18891–18897.

Wiedemann, F.R., Manfredi, G., Mawrin, C., Beal, M.F., and Schon, E.A. (2002). Mitochondrial DNA and respiratory chain function in spinal cords of ALS patients. J. Neurochem. *80*, 616–625.

Williamson, T.L., and Cleveland, D.W. (1999). Slowing of axonal transport is a very early event in the toxicity of ALS-linked SOD1 mutants to motor neurons. Nat. Neurosci. *2*, 50–56.

Wong, P.C., Pardo, C.A., Borchelt, D.R., Lee, M.K., Copeland, N.G., Jenkins, N.A., Sisodia, S.S., Cleveland, D.W., and Price, D.L. (1995). An adverse property of a familial ALS-linked SOD1 mutation causes motor neuron disease characterized by vacuolar degeneration of mitochondria. Neuron *14*, 1105–1116.

Xu, X., Decker, W., Sampson, M.J., Craigen, W.J., and Colombini, M. (1999). Mouse VDAC isoforms expressed in yeast: channel properties and their roles in mitochondrial outer membrane permeability. J. Membr. Biol. *170*, 89–102.

Yagoda, N., von Rechenberg, M., Zaganjor, E., Bauer, A.J., Yang, W.S., Fridman, D.J., Wolpaw, A.J., Smukste, I., Peltier, J.M., Boniface, J.J., et al. (2007). RAS-RAF-MEK-dependent oxidative cell death involving voltage-dependent anion channels. Nature *447*, 864–868.

Yamamoto, T., Yamada, A., Watanabe, M., Yoshimura, Y., Yamazaki, N., Yoshimura, Y., Yamauchi, T., Kataoka, M., Nagata, T., Terada, H., and Shinohara, Y. (2006). VDAC1, having a shorter N-terminus than VDAC2 but showing the same migration in an SDS-polyacrylamide gel, is the predominant form expressed in mitochondria of various tissues. J. Proteome Res. *5*, 3336–3344.

Yamanaka, K., Boillee, S., Roberts, E.A., Garcia, M.L., McAlonis-Downes, M., Mikse, O.R., Cleveland, D.W., and Goldstein, L.S. (2008a). Mutant SOD1 in cell types other than motor neurons and oligodendrocytes accelerates onset of disease in ALS mice. Proc. Natl. Acad. Sci. USA *105*, 7594–7599.

Yamanaka, K., Chun, S.J., Boillee, S., Fujimori-Tonou, N., Yamashita, H., Gutmann, D.H., Takahashi, R., Misawa, H., and Cleveland, D.W. (2008b). Astrocytes as determinants of disease progression in inherited amyotrophic lateral sclerosis. Nat. Neurosci. *11*, 251–253.

Yuan, S., Fu, Y., Wang, X., Shi, H., Huang, Y., Song, X., Li, L., Song, N., and Luo, Y. (2008). Voltage-dependent anion channel 1 is involved in endostatin-induced endothelial cell apoptosis. FASEB J. *22*, 2809–2820.

Zaid, H., Abu-Hamad, S., Israelson, A., Nathan, I., and Shoshan-Barmatz, V. (2005). The voltage-dependent anion channel-1 modulates apoptotic cell death. Cell Death Differ. *12*, 751–760.

Zamzami, N., and Kroemer, G. (2003). Apoptosis: mitochondrial membrane permeabilization—the (w)hole story? Curr. Biol. *13*, R71–R73.

Zheng, Y., Shi, Y., Tian, C., Jiang, C., Jin, H., Chen, J., Almasan, A., Tang, H., and Chen, Q. (2004). Essential role of the voltage-dependent anion channel (VDAC) in mitochondrial permeability transition pore opening and cytochrome c release induced by arsenic trioxide. Oncogene *23*, 1239–1247.

# ALSの病態

## ——非細胞自律性の神経細胞死

ALS：non-cell autonomous neuron death

山中宏二(写真)　遠藤史人
Koji YAMANAKA and Fumito ENDO
理化学研究所脳科学総合研究センター運動ニューロン変性研究チーム

◎筋萎縮性側索硬化症(ALS)の約10%は遺伝性に発症し，分子病態の研究はその遺伝子異常を再現したモデル動物の開発により進展してきた．遺伝性ALSのなかでもっとも頻度が高いSOD1優性変異を再現した変異SOD1トランスジェニックマウスは，運動ニューロンの選択的変性をきたすモデル動物として広く研究に用いられるようになった．変異SOD1モデルマウスを用いた研究で，ALSの運動ニューロン死は運動ニューロンに発現する変異蛋白質の毒性のみに起因するのではなく，その周囲のグリア細胞における病的変化も神経細胞死に深く関与することが解明された．このような非細胞自律性の神経細胞死とよばれる現象は，ALSだけでなく他の神経変性疾患においてもみられることが示されつつあり，神経疾患の研究動向に変化をもたらすものである．

Key word：SOD1，筋萎縮性側索硬化症(ALS)，グリア細胞，ミクログリア

筋萎縮性側索硬化症(ALS)の大半は孤発例であるが，約10%は遺伝性に発症する．そのなかでSOD1優性変異がもっとも多く総ALS患者の2%を占め，また最近発見された*TDP-43*変異，*FUS/TLS*変異は約1〜5%と報告により幅があるものの，やや頻度は低いと考えられる．1993年の遺伝性ALS家系における*SOD1*点変異の発見を機に，変異SOD1トランスジェニックマウスがALSの病態を再現するモデルとして樹立され，ALS研究は著しく進展した．

最近，TDP-43を手がかりに孤発性ALSの病態モデルの構築が進められているが，SOD1モデルのように選択性の運動ニューロン死が再現できるモデル動物の開発には至っていない．本稿では，変異SOD1によるALSモデルにおける細胞群ごとの病態解明と，グリア細胞の役割に関する研究動向をレビューする．

**サイドメモ　SOD1と変異SOD1毒性**

SOD1(Cu/Zn superoxide dismutase)は153アミノ酸からなる，細胞内で発生したスーパーオキシドラジカルを解毒化する酵素であり，細胞内では安定した二量体を形成している．疾患由来の変異SOD1蛋白質は，アミノ酸変異による可溶性の低下や構造変化によって病巣に蓄積している．変異SOD1蛋白による運動ニューロンに対する毒性発現の分子機構として，蛋白のフォールディング異常による凝集体形成，蛋白分解経路の異常，ミトコンドリア機能異常，酸化ストレス，軸索輸送の異常，シナプスにおけるグルタミン酸毒性，栄養因子の欠乏，グリア細胞に起因する神経炎症などが提唱されている[1]．ミスフォールドした変異SOD1蛋白質の病巣への蓄積は，SOD1変異を有する動物モデル，ヒト患者に共通して認められ，疾患形成に強く関与していると考えられている．

## 変異SOD1毒性

SOD1 優性変異をもつ ALS 患者では，現在までに 120 以上の異なる点変異と，C 末端を欠損した少数のフレームシフト変異が報告されている．変異 SOD1 を発現したトランスジェニックマウスは，運動ニューロンの変性による進行性の運動麻痺，筋萎縮を呈して ALS の病態を再現するのに対し，野生型 SOD1 を強発現したマウスや，SOD1 を欠失したマウスは運動ニューロン変性をきたさないことから，変異 SOD1 蛋白が本来の酵素活性と関係ない未知の毒性を発揮すること(gain of toxic function)が運動ニューロン変性の原因と考えられている[1](「サイドメモ」参照)，

## ALSにおける非細胞自律性の運動ニューロン死

SOD1 変異を有する ALS 患者やモデルマウス，さらに ALS 以外の多くの優性遺伝性神経変性疾患において，原因遺伝子がほとんどの細胞群に発現するが，系特異的な神経変性を認める．非神経細胞に発現する病因遺伝子産物の役割は不明であり，ALS 病巣でみられるアストロサイトの増殖やミクログリアの活性化が神経変性に伴う二次的変化なのか，または神経変性に直接貢献しているのかは未解明であった．当初，変異 SOD1 毒性は運動ニューロンに特異的であるとの仮説のもとに，神経細胞特異的に変異 SOD1 を発現するマウスが作成されたが，神経変性をきたさなかった[2,3]．

最近，神経細胞に変異 SOD1 を高発現するマウスの一部がきわめて late onset の疾患表現型を示すことが報告された[4]．これらの報告から変異 SOD1 毒性は運動ニューロン内でのみ惹起されるわけではないことが明らかとなった．その後，野生型マウスと ALS を発症する SOD1 マウスとのキメラマウスを用いた研究で，野生型細胞が多い環境にある変異 SOD1 を発現する運動ニューロンは長期生存することが示され，SOD1 マウスで起こる運動ニューロン変性は非細胞自律性(non-cell autonomous)に起こる，つまり神経変性は運動ニューロン由来の変異 SOD1 毒性のみで自律性に起こるのではなく，周囲の非神経細胞由来の変異 SOD1 毒性も必要であることが示された[5,6]．

## ALS発症および進行に関する細胞群の同定

### 1. 運動ニューロンにおける変異SOD1毒性はALSの発症を規定する

これらを踏まえて著者らは，どの細胞群に由来する変異 SOD1 毒性が神経変性に重要であるのかを解明するため，Cre-Lox システムを用い，細胞群特異的に除去可能な変異 SOD1 を発現するあらたなモデルマウス LoxSOD1$^{G37R}$を樹立した．LoxSOD1$^{G37R}$マウスはユビキタスに変異 SOD1 を発現し，進行性の運動ニューロン変性を再現した[7]．まず，運動ニューロンにおける変異 SOD1 毒性の役割を解明するため，運動ニューロン特異的に Cre 蛋白を発現するマウスと LoxSOD1$^{G37R}$マウスを交配し，運動ニューロン特異的に変異 SOD1 を除去すると，ALS の発症時期は遅延したものの，疾患進行の速度に変化はみられなかった[7,8]．また，SOD1$^{G85R}$マウスを用いて同様の実験を行ったグループも著者らと同様に発症時期の遅延を報告した[9]．これらの研究結果は，運動ニューロン特異的に RNA 干渉(RNA interference)を用いて変異 SOD1 の発現を抑制した場合，SOD1$^{G93A}$マウスの発症時期のみが著明に遅延したことと一致しており[10]，一連の実験結果から，運動ニューロンにおける変異 SOD1 毒性が ALS の発症時期を規定していると考えられる．

### 2. ミクログリアとアストロサイトはALSの進行を規定する細胞群である

ミクログリアはマクロファージに由来する中枢神経系の貪食細胞であり，ALS の進行につれてその活性化が病巣でみられる．ミクログリアは神経栄養性の因子を分泌する一方，炎症反応に関与する多くのサイトカインなども放出することが知られ，神経細胞にとって保護的である一方，神経傷害もきたすという両面性をもつ細胞群である[11]．そこで LoxSOD1$^{G37R}$マウスを CD11b-Cre マウスと交配してミクログリアに発現する変異 SOD1 を除去したところ，マウスの疾患進行を遅延して生存期間は著明に延長した[7]．同様の結果は SOD1$^{G85R}$マウスにおいても確認された[9]．また Appel らは，骨髄移植によって変異 SOD1 マウスのミクログリアおよびマクロファージを野生型に置換し，疾患進行を遅延させることに成功した[12]．

表 1　細胞群特異的な変異SOD1マウスおよび交配実験

| 細胞群 | マウス系統名，交配方法 | SOD1変異 | 発現 | 発症時期 | 疾患進行 | 生存期間 | 文献 |
|---|---|---|---|---|---|---|---|
| **(1) 細胞群特異的な強発現** | | | | | | | |
| ニューロン | トランスジェニックマウス (NF-L プロモーター) | G37R | ↑ | 発症せず | 発症せず | 発症せず | 2) |
| ニューロン | トランスジェニックマウス (Thy1 プロモーター) | G93A, G85R | ↑ | 発症せず | 発症せず | 発症せず | 3) |
| ニューロン | トランスジェニックマウス (Thy1.2 プロモーター) | G93A | ↑ | きわめて遅い | 緩徐 | 一部は死亡 | 4) |
| アストロサイト | トランスジェニックマウス (GFAP プロモーター) | G86R | ↑ | 発症せず | 発症せず | 発症せず (gliosis あり) | 21) |
| Schwann 細胞 | トランスジェニックマウス (P0 プロモーター) | G93A | ↑ | 発症せず | 発症せず | 発症せず | 22) |
| 骨格筋細胞 | トランスジェニックマウス (MLC プロモーター) | G93A | ↑ | 発症せず | 発症せず | 発症せず (筋力低下あり) | 23) |
| **(2) キメラマウスによる野生型細胞への置換** | | | | | | | |
| 全細胞群のキメラ | wild type::$SOD1^{G37R}$ | G37R | ↓ | 遅延 | 遅延 | 延長 | 5) |
| 運動ニューロン，oligodendrocyte 以外のキメラ | $Olig^{-/-}$::$SOD1^{G37R}$ | G37R | ↓ | 遅延 | 遅延 | 延長 | 6) |
| **(3) 細胞群特異的なノックダウン** | | | | | | | |
| 運動ニューロン | RNAi | G93A | ↓ | 遅延 | ほぼ不変 | 延長 | 10) |
| 運動ニューロン，後根神経節細胞 | $LoxSOD1^{G37R}$/Isl1-Cre | G37R | ↓ | 遅延 | 不変 | 延長 | 7) |
| 運動ニューロン | $LoxSOD1^{G37R}$/VAChT-Cre | G37R | ↓ | 遅延 | 不変 | 延長 | 8) |
| 運動ニューロン，介在ニューロン | $LoxSOD1^{G85R}$/Lhx3-Cre | G85R | ↓ | 遅延 | 不変 | 延長 | 9) |
| ミクログリア，マクロファージ | $LoxSOD1^{G37R}$/CD11b-Cre | G37R | ↓ | 不変 | 遅延 | 延長 | 7) |
| ミクログリア，マクロファージ | $LoxSOD1^{G85R}$/CD11b-Cre | G85R | ↓ | 不変 | 遅延 | 延長 | 9) |
| ミクログリア，マクロファージ | $SOD1^{G93A}$/$PU.1^{-/-}$，骨髄移植 | G93A | ↓ | 不変 | 遅延 | 延長 | 12) |
| アストロサイト | $LoxSOD1^{G37R}$/GFAP-Cre | G37R | ↓ | 不変 | 遅延 | 延長 | 8) |
| Schwann 細胞 | $LoxSOD1^{G37R}$/P0-Cre | G37R | ↓ | 不変 | 短縮 | 短縮 | 18) |
| 骨格筋細胞 | $LoxSOD1^{G37R}$/MCK-Cre | G37R | ↓ | 不変 | 不変 | 不変 | 17) |
| 骨格筋細胞，(少数の運動ニューロン) | RNAi | G93A | ↓ | 不変 | 不変 | 不変 | 24) |
| 血管内皮細胞 | $LoxSOD1^{G37R}$/Ve-Cadherin-$Cre^{+}$ | G37R | ↓ | 不変 | 不変 | 不変 | 20) |

細胞群特異的な変異 SOD1 毒性は，①細胞群特異的に変異 SOD1 を発現する方法，②キメラマウス作成，③細胞群特異的な変異 SOD1 ノックダウンにより行われてきた．スペースの制約で，本稿中で解説できなかった研究も含め，その結果の要点を示す．①では単一細胞群での強発現により ALS 様の表現型を示したかどうか，②③ではユビキタスに変異 SOD1 遺伝子を発現するモデルマウスと比較して発症，進行，生存期間に影響があるかが焦点となる．

これらの実験結果はミクログリアにおける病的変化が ALS の疾患進行を規定することを示し，ミクログリアを正常化することが ALS 治療標的となることが期待される．さらに最近では，ALS モデルの神経変性に T 細胞の関与が報告され，免疫系とグリア細胞との機能連関がトピックスとなっている[13]．

アストロサイトは神経細胞に栄養因子を供給するのみならず，シナプス活動の調節など多岐にわたる機能をもつグリア細胞である．そこで，$LoxSOD1^{G37R}$を用いてアストロサイト特異的に変異 SOD1 を除去すると，ミクログリアの異常な活性化を抑制し，発症後の進行を約 2.2 倍延長して生存期間を著明に延長した[8]．また，*in vitro* の実験系で，変異 SOD1 を発現するアストロサイトは運動ニューロンに対して毒性を発揮することも示された[14,15]．さらに，野生型のグリア幹細胞を変異 SOD1 ラットの頸髄に移植することにより疾患進行を遅延させた研究が発表され[16]，グリア細胞が実行する非細胞自律性の神経細胞死という概念が

多くの研究により実証されている．

つまり，ALSの発症は運動ニューロンに蓄積するさまざまな病的変化に起因するが，その進行はアストロサイトとミクログリアに起因する病的変化が深く関与し，アストロサイトがミクログリアをより活性化させ，細胞障害性サイトカインなどの放出を促進して運動ニューロン変性を加速すると考えられる．

## その他の細胞群

### ——Schwann細胞，骨格筋，血管内皮細胞

LoxSOD1$^{G37R}$マウスを用いて骨格筋に発現する変異SOD1の効果が検討されたが，ALS発症や進行への関与が認められなかった[17]．これに対してSchwann細胞特異的にSOD1酵素活性をもつSOD1G37Rを除去すると疾患進行がかえって加速した[18]．Schwann細胞では酸化ストレスの除去が神経保護的に作用する可能性が考えられる．ALSモデルマウスの脊髄において血管内皮の脆弱性から微小出血を起こすことが示され，また患者病巣においてもタイトジャンクションの構成分子ZO-1，occludinのmRNA発現低下が確認されている[19]．しかし，LoxSOD1$^{G37R}$マウスを用いて血管内皮細胞からの変異SOD1を除去しても，疾患の発症や進行への影響はみられなかった[20]．

これまでに，動物モデルの作成を通じて細胞群特異的な変異SOD1の役割を解析した結果が多数報告されており，ここにまとめて紹介する(表1)．このように，神経変性疾患の病態解明において障害されるニューロンだけではなく，その周囲の細胞群の病態も検討することの重要性が認識されてきている．

## おわりに

神経難病のなかでももっとも克服が難しいと考えられていたALSにおいても，近年の研究の著しい進歩により希望の光がみえつつある．また，孤発性神経変性疾患の治療は発症後に行われ，疾患の進行を遅延させることが治療目標となるため，疾患の進行を規定する因子の検索は非常に重要である．ALSの疾患進行を規定する細胞群として同定されたグリア細胞であるミクログリアやアストロサイトは，まさにALS治療の標的として有望である．グリア細胞の分子病態を解明し，さらにグリア幹細胞によるcell replacement therapyや，薬剤投与などの方法により，運動ニューロンではなく，その周囲の非神経細胞であるグリア細胞を正常化することによるALS治療が将来可能になることが期待される．

## 文献


1) Ilieva, H. et al.：Non-cell autonomous toxicity in neurodegenerative disorders：ALS and beyond. *J. Cell Biol.*, **187**：761-772, 2009.
2) Pramatarova, A. et al.：Neuron-specific expression of mutant superoxide dismutase 1 in transgenic mice does not lead to motor impairment. *J. Neurosci.*, **21**：3369-3374, 2001.
3) Lino, M. M. et al.：Accumulation of SOD1 mutants in postnatal motoneurons does not cause motoneuron pathology or motoneuron disease. *J. Neurosci.*, **22**：4825-4832, 2002.
4) Jaarsma, D. et al.：Neuron-specific expression of mutant superoxide dismutase is sufficient to induce amyotrophic lateral sclerosis in transgenic mice. *J. Neurosci.*, **28**：2075-2088, 2008.
5) Clement, A. M. et al.：Wild-type nonneuronal cells extend survival of SOD1 mutant motor neurons in ALS mice. *Science*, **302**：113-117, 2003.
6) Yamanaka, K. et al.：Mutant SOD1 in cell types other than motor neurons and oligodendrocytes accelerates onset of disease in ALS mice. *Proc. Natl. Acad. Sci. USA*, **105**：7594-7599, 2008.
7) Boillee, S. et al.：Onset and progression in inherited ALS determined by motor neurons and microglia. *Science*, **312**：1389-1392, 2006.
8) Yamanaka, K. et al.：Astrocytes as determinants of disease progression in inherited amyotrophic lateral sclerosis. *Nat. Neurosci.*, **11**：251-253, 2008.
9) Wang, L. et al.：The effect of mutant SOD1 dismutase activity on non-cell autonomous degeneration in familial amyotrophic lateral sclerosis. *Neurobiol. Dis.*, **35**：234-240, 2009.
10) Ralph, G. S. et al.：Silencing mutant SOD1 using RNAi protects against neurodegeneration and extends survival in an ALS model. *Nat. Med.*, **11**：429-433, 2005.
11) Sargsyan, S. A. et al.：Microglia as potential contributors to motor neuron injury in amyotrophic lateral sclerosis. *Glia*, **51**：241-253, 2005.
12) Beers, D. R. et al.：Wild-type microglia extend survival in PU. 1 knockout mice with familial amyotrophic lateral sclerosis. *Proc. Natl. Acad. Sci. USA*, **103**：16021-16026, 2006.
13) Beers, D. R. et al.：CD4$^{+}$T cells support glial neuroprotection, slow disease progression, and modify glial morphology in an animal model of inherited ALS. *Proc. Natl. Acad. Sci. USA*, **105**：15558-15563, 2008.
14) Nagai, M. et al.：Astrocytes expressing ALS-

linked mutated SOD1 release factors selectively toxic to motor neurons. *Nat. Neurosci.*, **10** : 615-622, 2007.
15) Di Giorgio, F. P. et al. : Human embryonic stem cell-derived motor neurons are sensitive to the toxic effect of glial cells carrying an ALS-causing mutation. *Cell Stem Cell*, **3** : 637-648, 2008.
16) Lepore, A. C. et al. : Focal transplantation-based astrocyte replacement is neuroprotective in a model of motor neuron disease. *Nat. Neurosci.*, **11** : 1294-1301, 2008.
17) Miller, T. M. et al. : Gene transfer demonstrates that muscle is not a primary target for non-cell-autonomous toxicity in familial amyotrophic lateral sclerosis. *Proc. Natl. Acad. Sci. USA*, **103** : 19546-19551, 2006.
18) Lobsiger, C. S. et al. : Schwann cells expressing dismutase active mutant SOD1 unexpectedly slow disease progression in ALS mice. *Proc. Natl. Acad. Sci. USA*, **106** : 4465-4470, 2009.
19) Henkel, J. S. et al. : Decreased mRNA expression of tight junction proteins in lumbar spinal cords of patients with ALS. *Neurology*, **72** : 1614-1616, 2009.
20) Zhong, Z. et al. : Activated protein C therapy slows ALS-like disease in mice by transcriptionally inhibiting SOD1 in motor neurons and microglia cells. *J. Clin. Invest.*, **119** : 3437-3449, 2009.
21) Gong, Y. H. et al. : Restricted expression of G86R Cu/Zn superoxide dismutase in astrocytes results in astrocytosis but does not cause motoneuron degeneration. *J. Neurosci.*, **20** : 660-665, 2000.
22) Turner, B. J. et al. : Dismutase-competent SOD1 mutant accumulation in myelinating Schwann cells is not detrimental to normal or transgenic ALS model mice. *Hum. Mol. Genet.*, **19** : 815-824, 2010.
23) Dobrowolny, G. et al. : Skeletal muscle is a primary target of SOD1G93A-mediated toxicity. *Cell Metab.*, **8** : 425-436, 2008.
24) Towne, C. et al. : Systemic AAV6 delivery mediating RNA interference against SOD1 : neuromuscular transduction does not alter disease progression in fALS mice. *Mol. Ther.*, **16** : 1018-1025, 2008.

*　　*　　*

doi:10.1038/nature08971

nature

LETTERS

# Mutations of optineurin in amyotrophic lateral sclerosis

Hirofumi Maruyama[1], Hiroyuki Morino[1], Hidefumi Ito[2]†, Yuishin Izumi[3], Hidemasa Kato[4], Yasuhito Watanabe[5], Yoshimi Kinoshita[2], Masaki Kamada[1,3], Hiroyuki Nodera[3], Hidenori Suzuki[6], Osamu Komure[7], Shinya Matsuura[8], Keitaro Kobatake[9], Nobutoshi Morimoto[10], Koji Abe[10], Naoki Suzuki[11], Masashi Aoki[11], Akihiro Kawata[12], Takeshi Hirai[12], Takeo Kato[13], Kazumasa Ogasawara[14], Asao Hirano[15], Toru Takumi[5], Hirofumi Kusaka[2], Koichi Hagiwara[16], Ryuji Kaji[3] & Hideshi Kawakami[1]

**Amyotrophic lateral sclerosis (ALS) has its onset in middle age and is a progressive disorder characterized by degeneration of motor neurons of the primary motor cortex, brainstem and spinal cord[1]. Most cases of ALS are sporadic, but about 10% are familial. Genes known to cause classic familial ALS (FALS) are superoxide dismutase 1 (*SOD1*)[2], *ANG* encoding angiogenin[3], *TARDP* encoding transactive response (TAR) DNA-binding protein TDP-43 (ref. 4) and fused in sarcoma/translated in liposarcoma (*FUS*, also known as *TLS*)[5,6]. However, these genetic defects occur in only about 20–30% of cases of FALS, and most genes causing FALS are unknown. Here we show that there are mutations in the gene encoding optineurin (*OPTN*), earlier reported to be a causative gene of primary open-angle glaucoma (POAG)[7], in patients with ALS. We found three types of mutation of *OPTN*: a homozygous deletion of exon 5, a homozygous Q398X nonsense mutation and a heterozygous E478G missense mutation within its ubiquitin-binding domain. Analysis of cell transfection showed that the nonsense and missense mutations of *OPTN* abolished the inhibition of activation of nuclear factor kappa B (NF-κB), and the E478G mutation revealed a cytoplasmic distribution different from that of the wild type or a POAG mutation. A case with the E478G mutation showed OPTN-immunoreactive cytoplasmic inclusions. Furthermore, TDP-43- or SOD1-positive inclusions of sporadic and *SOD1* cases of ALS were also noticeably immunolabelled by anti-OPTN antibodies. Our findings strongly suggest that OPTN is involved in the pathogenesis of ALS. They also indicate that NF-κB inhibitors could be used to treat ALS and that transgenic mice bearing various mutations of *OPTN* will be relevant in developing new drugs for this disorder.**

We analysed six Japanese individuals from consanguineous marriages who had ALS; two of them were siblings, the others were from independent families. We used homozygosity mapping, which has been shown to identify a locus of a disease-causing gene from as few as three individuals[8]. We performed a genome-wide scan of single nucleotide polymorphisms (SNPs) by using the GeneChip Human Mapping 500K Array Set (Affymetrix), and selected for the run of homozygous SNPs (RHSs) more than 3 centimorgans in length. Under this condition, the RHSs are able to retrieve more than 98% of the entire length of the autozygous segments created as a result of a first-cousin or second-cousin marriage (Supplementary Information)[8]. We extracted RHSs of six individuals (Supplementary Fig. 1a). A region (hg18: 12,644,480–15,110,539) in chromosome 10, which was an overlap among four subjects, was chosen as the primary candidate region (Supplementary Fig. 1b). Assuming that subjects ii, iii, v and vi had the same disease gene, the chance that the overlap had the disease gene was $P_{ii+iii+v+vi} = 0.935$ (Supplementary Information). We listed up to 17 candidate genes in the region and sequenced their exons (Supplementary Fig. 1c). We detected a deletion of exon 5 in the *OPTN* (also known as FIP-2 (ref. 9)) gene in two siblings (Fig. 1a, family 1, subjects 1 and 2). PCR with a forward primer of exon 4 and a reverse primer of intron 5 revealed a 2.5-kilobase (kb) band in the control, V-3 and IV-1, and a 0.7-kb band in IV-1, subject 1 and subject 2 (Fig. 1b). Direct sequence analysis of the short band showed the joining of the 5′ part of AluJb in intron 4 and the 3′ part of AluSx in intron 5 with 12-base-pair (bp) microhomology (Fig. 1c). Thus, the deletion resulted from Alu-mediated recombination. We also found a homozygous nonsense c.1502C>T mutation (Q398X, exon 12) in the gene in one individual with ALS (Fig. 1d, e, family 2, subject 3). For the other three subjects, we found neither mutations nor copy number changes in the *OPTN* gene, although we did not completely exclude the possibility of mutations in introns or intergenic regions in the gene. We extended our analysis of *OPTN* to ten additional individuals from consanguineous marriages who had ALS, 76 individuals with familial ALS and 597 individuals with sporadic ALS (SALS). We found the Q398X mutation in a sporadic individual (subject 4, family 3; Fig. 1d). Subjects 3 and 4, who were not related according to their family history, shared their haplotype for a 0.9-megabase (Mb) region (hg18: chr10: 12,973,261–13,879,735) containing the *OPTN* gene (Supplementary Table 1). We investigated a total of 170 copies of chromosome 10 from 85 Japanese subjects genotyped for the HapMap3 project, and found that the incidental length of haplotype sharing around *OPTN* gene was at most 320 kb. Given that a haplotype sharing of 0.9 Mb rarely occurs by chance, the mutation is likely to have been derived from a single ancestor (Supplementary Fig. 1d). Subjects 1 and 2 shared their homozygous haplotype for an 8.3-Mb region

[1]Department of Epidemiology, Research Institute for Radiation Biology and Medicine, Hiroshima University, Hiroshima 734-8553, Japan. [2]Department of Neurology, Kansai Medical University, Moriguchi 570-8506, Japan. [3]Department of Clinical Neuroscience, University of Tokushima Graduate School, Tokushima 770-8503, Japan. [4]Division of Developmental Biology, Research Center for Genomic Medicine, Saitama Medical University, Saitama 350-1241, Japan. [5]Laboratory of Integrative Bioscience, Hiroshima University Graduate School of Biomedical Sciences, Hiroshima 734-8551, Japan. [6]Faculty of Human Science, Hiroshima Bunkyo Women's University, Hiroshima 731-0295, Japan. [7]South Osaka Neurosurgical Hospital, Osakasayama 589-0011, Japan. [8]Department of Radiation Biology, Research Institute for Radiation Biology and Medicine, Hiroshima University, Hiroshima 734-8553, Japan. [9]Department of Neurology, Kobatake Hospital, Fukuyama 720-1142, Japan. [10]Department of Neurology, Okayama University, Graduate School of Medicine, Dentistry, and Pharmaceutical Sciences, Okayama 700-8558, Japan. [11]Department of Neurology, Tohoku University School of Medicine, Sendai 980-8574, Japan. [12]Department of Neurology, Tokyo Metropolitan Neurological Hospital, Fuchu, Tokyo 183-0042, Japan. [13]Department of Neurology, Haematology, Metabolism, Endocrinology and Diabetology, Yamagata University Faculty of Medicine, Yamagata 990-9585, Japan. [14]Department of Pathology, School of Medicine, Shiga University of Medical Science, Ohtsu 520-2192, Japan. [15]Division of Neuropathology, Department of Pathology, Montefiore Medical Center, New York, New York 10467-2490, USA. [16]Department of Respiratory Medicine, Saitama Medical University, Saitama 350-0495, Japan. †Present address: Department of Neurology, Kyoto University Graduate School of Medicine, Kyoto 606-8507, Japan.

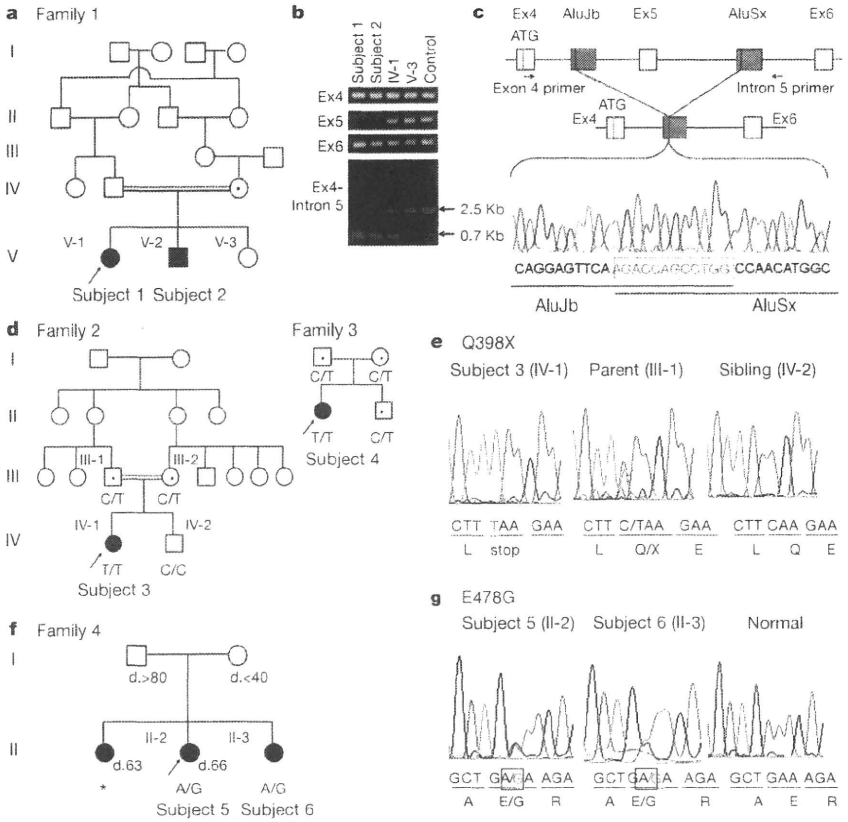


**Figure 1 | Exon 5 deletion, nonsense and missense mutations of the *OPTN* gene. a**, Family 1. The filled circle or square indicate the affected individuals; the arrows indicate the probands. **b**, Agarose gel electrophoretogram. Subject 1 (V-1) and subject 2 (V-2) showed lack of exon 5 PCR product and shortened product of exon 4 to intron 5. **c**, Chromatogram with OPTN deletion of exon 5 and schematic structure of deleted gene. **d**, Families 2 and 3. Dots indicate heterozygous carriers. **e**, Chromatograms from index subjects with OPTN mutation of c.1502 C>T. Homozygous mutation is in red, and the mutation is indicated by using the single-letter amino-acid code. **f**, Family 4. *DNA sample could not be obtained. Numerals show the age at death. **g**, Chromatograms from index subjects with the OPTN mutation of c.1743A>G. The heterozygous mutation is marked by the square.

(hg18: chr10: 6,815,934–14,842,351), which contained the *OPTN* gene and was different from that in subjects 3 and 4 (Supplementary Table 1).

In the screening of ALS families, we identified a heterozygous missense mutation (c1743A>G, E478G, exon14, Fig. 1g) of *OPTN* in four individuals with ALS in two families with ALS. Subjects 5 and 6 were sisters, and the pedigree suggests that the mutation had an autosomal dominant trait with incomplete penetrance (Fig. 1f, family 4). Subjects 7 and 8 (family 5) were brothers. Although these families are not related according to their family history, subjects 5–8 shared their haplotype for 2.3 Mb (hg18: chr10: 11,460,985–13,703,017, Supplementary Table 3), again suggesting that the mutation was derived from a single ancestor. Indeed, the Q398X nonsense and E478G missense mutations were not observed in 781 healthy Japanese volunteers as well as in over 6,800 (including 1,728 Japanese) individuals in the glaucoma studies, where the entire coding region of the gene was investigated (Supplementary Table 2). Collectively, the mutation was absent over a total of 5,000 Japanese chromosomes. The deletion mutation was also absent in 200 Japanese, and not reported in the over 6,800 glaucoma individuals. The co-segregation of three different mutations of *OPTN* with the ALS phenotype strongly suggests that some mutations of *OPTN* cause ALS.

The eight individuals with mutations of *OPTN* showed onset from 30 to 60 years of age. Most of them showed a relatively slow progression and long duration before respiratory failure, although the clinical phenotypes were not homogeneous (see Supplementary Information).

The Q398X mutation causes a premature stop during translation, truncating the 577 amino-acid OPTN protein to one of 397 amino acids in length. This truncation results in a deletion of the coiled coil 2 domain[10], which is necessary for binding to ubiquitin[11], huntingtin[12], myosin VI[13] and the ubiquitinated receptor-interacting protein[14]. In the gene with the deletion of exon 5, if there was a transcript, the transcript splicing from exon 4 to exon 6 would cause a frame shift and make a stop codon (TGA in the ninth to eleventh codons in exon 6), which would be expected to translate a peptide 58 amino acids in length. The missense mutation (E478G) was located between coiled coil 2 domain and the leucine zipper domain. This glutamic acid is highly conserved among OPTN proteins of a wide range of species (Supplementary Fig. 2a), and is situated within the DFxxER motif, an ubiquitin-binding domain shared among OPTN, NF-κB essential molecule (NEMO), and A20 binding and inhibitor of NF-κB proteins (ABIN) (Supplementary Fig. 2b). The mutations in the DFxxER motif in ABIN reduce the binding to ubiquitin, which render them unable to inhibit NF-κB activation[11]. We investigated the ability of various mutations of *OPTN* to inhibit NF-κB-mediated transcriptional activation by performing a luciferase assay using NSC-34 cells (a mouse neuroblastoma and spinal-cord hybrid cell line) transfected with wild-type or mutant *OPTN*. E50K *OPTN*, which causes POAG[7], downregulated the NF-κB activity, as did the wild type. On the other hand, both Q398X and E478G had no ability to inhibit NF-κB activity (Tukey–Kramer, $P < 0.05$). These tendencies were retained after stimulation with tumour-necrosis factor (TNF)-α (Fig. 2A). We also examined the subcellular localization of overexpressed Flag-tagged wild-type OPTN (wild type) and its mutants in cells (Fig. 2B).

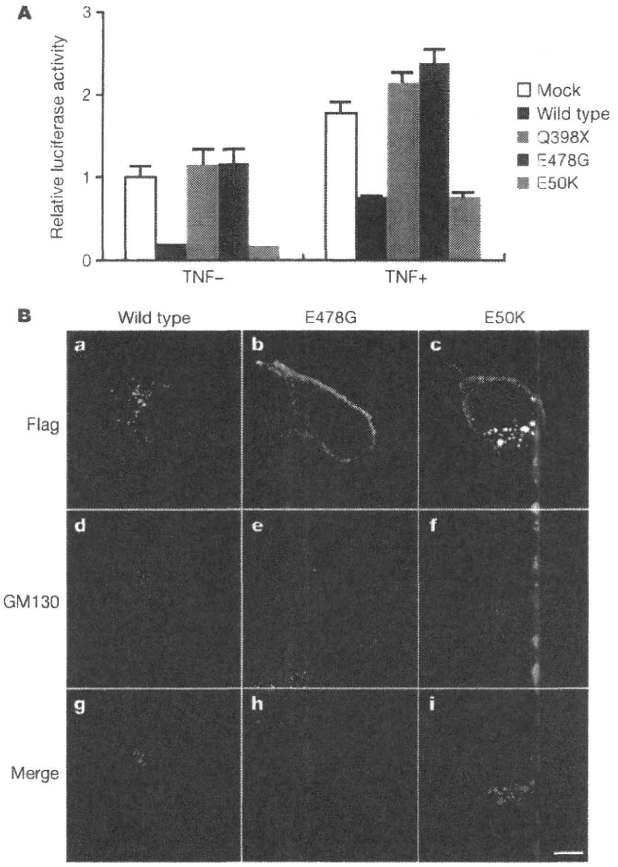


**Figure 2 | Influence of OPTN mutations. A**, Luciferase assay to assess the ability of various OPTNs to inhibit activation of NF-κB. The wild type and E50K have a similar NF-κB activation-inhibiting effect, whereas mock, Q398X and E478G types lack this effect. Error bars, standard deviations of triplicate assays. **B**, Localization of OPTN. Flag is the white signals in a–c and red signals in g–i. GM130 is the white signals in d–f and green signals in g–i. The wild type shows many fluorescent granules co-localized with the Golgi apparatus. E478G OPTN shows a reduced number of granules, and rarely co-localized with the Golgi apparatus. E50K OPTN granules have become large and co-localized with the Golgi apparatus. Scale bar, 10 μm.

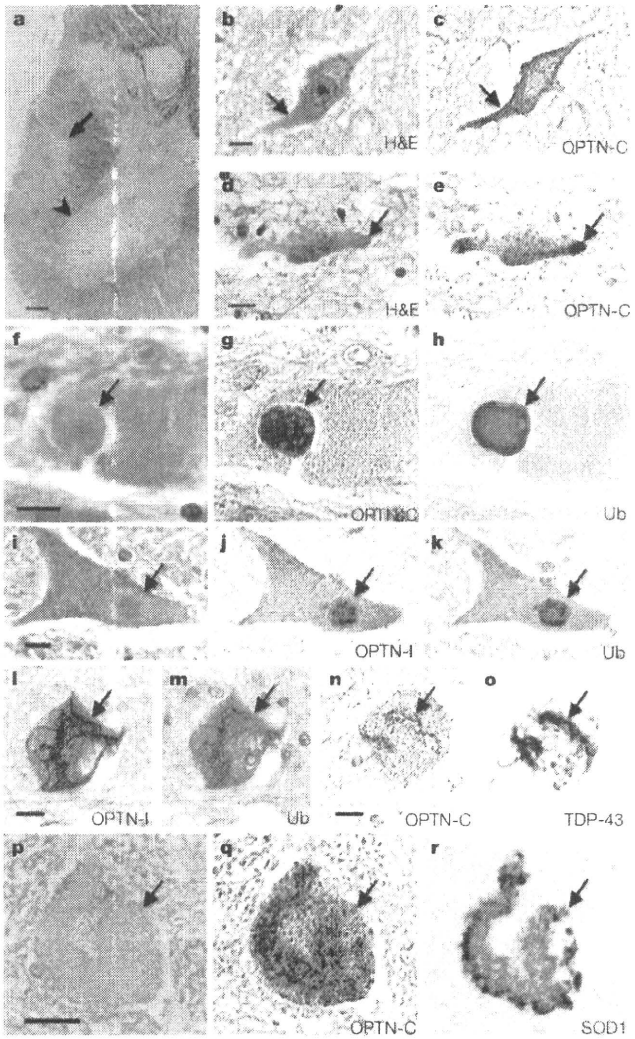


**Figure 3 | Identification of OPTN in distinctive intracytoplasmic inclusions of subjects with ALS. a–e**, Neuropathology of the lumbar spinal cord from subject 5. Klüver-Barrera (**a**) show loss of myelin from the corticospinal tract (arrow) and loss of motor neurons from the anterior horn (arrowhead). The cytoplasm of the remaining motor neurons contains an amorphous eosinophilic region (**b**, arrow). H&E, haematoxylin and eosin. The same neuron was re-stained with the anti-OPTN antibody (**c**, arrow). The eosinophilic retention occasionally appears to form a hyaline inclusion (**d**, arrow), which is intensely immunolabelled with the anti-OPTN antibody (**e**, arrow). **f–k**, Round hyaline inclusions of subjects with SALS (**f**, **i**) are immunolabelled with anti-OPTN-C and anti-OPTN-I antibodies (**g** and **j**, respectively). The sections were re-stained with anti-ubiquitin (Ub) antibodies (**h**, **k**). **l–o**, Skein-like inclusions of patients with SALS are reactive with the anti-OPTN-I and anti-OPTN-C antibodies (**l**, **n**). Re-staining of **l** with the anti-ubiquitin antibody (**m**) and **n** with anti-TDP-43 antibody (**o**). **p–r**, Lewy-body-like hyaline inclusion of a patient with FALS, stained with haematoxylin and eosin (**p**), anti-OPTN-C antibody (**q**) and SOD1 antibody (**r**). Scale bars, 200 μm (**a**), 20 μm (**b–p**).

Immunofluorescence staining was performed with their antibodies against Flag and the Golgi matrix marker GM130. Confocal images showed close apposition of granular signals of wild-type OPTN or E50K with GM130 (see g and i in Fig. 2B)[15,16]. E50K often shapes large granular structures near the Golgi apparatus. E478G rarely showed granular signals (see b in Fig. 2B); however, when closely observed, some of the signals were still closely localized to GM130 (see h in Fig. 2B). Western blotting using a lysate of transformed lymphoblasts showed that the 74-kDa band, corresponding to OPTN, was absent in subjects 3 and 4, but was present in the non-diseased mother and brother of subject 3 (Supplementary Fig. 3a). Quantitative PCR with reverse transcription revealed that the products were diminished to 58.0% in the heterozygote (III-2) and to 13.8% in the homozygote (subject 4) compared with the control levels (Supplementary Fig. 3b). In addition, cycloheximide recovered the decrease in the OPTN messenger RNA (mRNA) with the mutation (Supplementary Fig. 3c). Thus mRNA with this mutation, which bears a premature termination, might be degraded through nonsense-mediated mRNA decay in lymphoblasts.

The spinal cord from subject 5 with the E478G mutation revealed loss of myelin from the corticospinal tract and of the anterior horn cells (AHCs, Fig. 3a and Supplementary Fig. 4a, b). OPTN immunohistochemistry demonstrated increased staining intensity of the cytoplasm of the remaining AHCs and the neurites in the anterior horn (Supplementary Fig. 4c). Higher magnification of the motor neurons revealed intracytoplasmic eosinophilic inclusions (Fig. 3b, d). Intriguingly, these inclusions were distinctly immunopositive for OPTN (Fig. 3c, e). On the other hand, the cytoplasm of AHCs from control individuals was faintly labelled with anti-OPTN antibodies (Supplementary Fig. 5a, c), similar to the spinal-cord AHCs of mice (Supplementary Fig. 6b) and in contrast to the highly labelled sensory

neurons in the dorsal root ganglia of mice (Supplementary Fig. 6d). In patients with sporadic ALS, the staining intensity for OPTN apparently increased not only in the cytoplasm of the remaining AHCs but also in their neurites (Supplementary Fig. 5b, d). In addition, distinctive intracytoplasmic inclusions were also noticeably OPTN immunolabelled in cases of sporadic and familial ALS; eosinophilic round hyaline inclusions from patients with SALS were immunopositive for OPTN (Fig. 3f, g, i, j). Re-staining of the same sections for ubiquitin, a known constituent of many neurodegenerative inclusions, revealed that these inclusions were also positive and faithfully matched the distribution of OPTN immunoreactivity (Fig. 3h, k). The anti-OPTN antibodies also stained skein-like inclusions (Fig. 3l, n), which were again mirrored with the anti-ubiquitin antibodies (Fig. 3m) and with the anti-TDP-43 antibodies (Fig. 3o). The distinct OPTN immunoreactivity of ubiquitin- and TDP-43-positive intracytoplasmic inclusions was confirmed on serial sections from patients with SALS (Supplementary Fig. 7). Moreover, SOD1-immunopositive Lewy-body-like hyaline inclusions from cases with *SOD1* FALS were also immunopositive for OPTN (Fig. 3p–r). We found that OPTN antibody labelled both SOD1- and TDP-43-positive inclusions. As the staining of SOD1 and TDP-43 is generally mutually exclusive, OPTN staining appears to be a more general marker for inclusions in various types of ALS; therefore, the OPTN molecule might also be involved in a broader pathogenesis of ALS.

The mutations of the *OPTN* gene cause both recessive and dominant traits, and the mechanism causing the disease may be different between the two traits. The Q398X nonsense mutation and probably the exon 5 deletion mutation cause a decrease in OPTN expression resulting from nonsense-mediated mRNA decay of the transcript carrying the nonsense OPTN mutations. Therefore, the mutated OPTN protein by itself is unlikely to disturb cell function or to be included in the inclusion body in the motor neuron cells. The mechanism of recessive mutations causing ALS is expected to be simply loss of function, and the heterozygote for the Q398X mutation does not develop the ALS phenotype. On the other hand, the E478G missense mutation increased the immunoreactivity for OPTN in the cell body and the neurites. The increased amount and different distribution of the mutated protein would disturb neuronal functions, and may accelerate the inclusion body formation as well as the increase and the different distribution of OPTN immunoreactivity in sporadic ALS. Thus the heterozygote for the E478G mutation will develop the disease.

The different impact on NF-κB signalling and the different intracellular localization of ALS- and POAG-linked mutated protein may explain the phenotypic divergence between the two diseases. Subject 3 with homozygotic Q398X also showed POAG, whereas subject 4 with the same mutation, and subjects 1 and 2 with the exon 5 deletion, did not show it. The prevalence of POAG in the population older than 40 years is 3.9% in Japan[17].Considering this information, the ALS and glaucoma in subject 3 may accidentally coexist.

OPTN competes with NF-κB essential molecule for binding to the ubiquitinated receptor-interacting protein and negatively regulates TNF-α-induced activation of NF-κB[14], which mediates an upregulation of OPTN, creating a negative feedback loop[18]. ALS-related OPTN mutations lacked the inhibitory effect towards NEMO, and thus exaggerated NF-κB activation. In sporadic ALS, a previous report showed that NF-κB, which is classified as a 'cell death inhibitor', is upregulated in motor neurons[19]. The upregulated NF-κB may induce the overexpression of OPTN, and may also cause neuronal cell death[20]. Thus NF-κB is a major candidate target for treating this disease. Additionally OPTN plays an important role in the maintenance of the Golgi complex, in membrane trafficking, in exocytosis, through its interaction with myosin VI and Rab8 (ref. 13), and in post-Golgi trafficking to lysosomes dependent on the Rab8/OPTN/htt complex[21] (Supplementary Fig. 8). Interestingly, FUS/TLS has been reported to interact with myosin VI[22] as well as with myosin V[23]. Impairment of intracellular trafficking of the complex including OPTN and/or FUS/TLS may cause inclusions in this neurodegenerative disorder.

## METHODS SUMMARY

**Genotyping and extraction of candidate regions.** The genotype of the GeneChip Human Mapping 500K Array Set (Affymetrix) was performed by AROS Applied Biotechnology. Computer analyses of the SNPs were performed by a homozygosity mapping algorithm accommodated to the whole-genome SNP scan data (Supplementary Information). To investigate the existence of a large insertion or deletion in this region, we analysed the copy number using Affymetrix Genotyping Console version 4.0 for the Affymetrix Mapping 500K data.

**Full Methods** and any associated references are available in the online version of the paper at www.nature.com/nature.

**Received 17 August 2009; accepted 2 March 2010.**
**Published online XX 2010.**

1. Leigh, P. N. in *Handbook of Clinical Neurology: Amyotrophic Lateral Sclerosis* Vol. 82 (eds Eisen, A. A. & Shaw, P. J.) 249–278 (Elsevier, 2007).
2. Rosen, D. R. *et al.* Mutations in Cu/Zn superoxide dismutase gene are associated with familial amyotrophic lateral sclerosis. *Nature* 362, 59–62 (1993).
3. Greenway, M. J. *et al. ANG* mutations segregate with familial and 'sporadic' amyotrophic lateral sclerosis. *Nature Genet.* 38, 411–413 (2006).
4. Sreedharan, J. *et al.* TDP-43 mutations in familial and sporadic amyotrophic lateral sclerosis. *Science* 319, 1668–1672 (2008).
5. Kwiatkowski, T. J. *et al.* Mutations in the *FUS/TLS* gene on chromosome 16 cause familial amyotrophic lateral sclerosis. *Science* 323, 1205–1208 (2009).
6. Vance, C. *et al.* Mutations in FUS, an RNA processing protein, cause familial amyotrophic lateral sclerosis type 6. *Science* 323, 1208–1211 (2009).
7. Rezaie, T. *et al.* Adult-onset primary open-angle glaucoma caused by mutations in optineurin. *Science* 295, 1077–1079 (2002).
8. Huqun, et a. l. Mutations in the SLC34A2 gene are associated with pulmonary alveolar microlithiasis. *Am. J. Respir. Crit. Care Med.* 175, 263–268 (2007).
9. Li, Y., Kang, J. & Horwitz, M. S. Interaction of an adenovirus E3 14.7-kilodalton protein with a novel tumor necrosis factor alpha-inducible cellular protein containing leucine zipper domains. *Mol. Cell. Biol.* 18, 1601–1610 (1998).
10. Schwamborn, K., Weil, R., Courtois, G., Whiteside, S. T. & Israël, A. Phorbol esters and cytokines regulate the expression of the NEMO-related protein, a molecule involved in a NF-κB-independent pathway. *J. Biol. Chem.* 275, 22780–22789 (2000).
11. Wagner, S. *et al.* Ubiquitin binding mediates the NF-κB inhibitory potential of ABIN proteins. *Oncogene* 27, 3739–3745 (2008).
12. Hattula, K. & Peränen, J. FIP-2, a coiled-coil protein, links huntingtin to Rab8 and modulates cellular morphogenesis. *Curr. Biol.* 10, 1603–1606 (2000).
13. Sahlender, D. A. *et al.* Optineurin links myosin VI to the Golgi complex and is involved in Golgi organization and exocytosis. *J. Cell Biol.* 169, 285–295 (2005).
14. Zhu, G., Wu, C. J. & Ashwell, J. D. Optineurin negatively regulates TNFα-induced NF-κB activation by competing with NEMO for ubiquitinated RIP. *Curr. Biol.* 17, 1438–1443 (2007).
15. De Marco, N., Buono, M., Troise, F. & Diez-Roux, G. Optineurin increases cell survival and translocates to the nucleus in a Rab8-dependent manner upon an apoptotic stimulus. *J. Biol. Chem.* 281, 16147–16156 (2006).
16. Chalasani, M. L., Balasubramanian, D. & Swarup, G. Focus on molecules: optineurin. *Exp. Eye Res.* 87, 1–2 (2008).
17. Iwase, A. *et al.* The prevalence of primary open-angle glaucoma in Japanese: the Tajimi Study. *Ophthalmology* 111, 1641–1648 (2004).
18. Mrowka, R., Blüthgen, N. & Fähling, M. Seed-based systematic discovery of specific transcription factor target genes. *FEBS J.* 275, 3178–3192 (2008).
19. Jiang, Y. M. *et al.* Gene expression profile of spinal motor neurons in sporadic amyotrophic lateral sclerosis. *Ann. Neurol.* 57, 236–251 (2005).
20. Pizzi, M. & Spano, P. Distinct roles of diverse nuclear factor-κB complexes in neuropathological mechanisms. *Eur. J. Pharmacol.* 545, 22–28 (2006).
21. Toro, D. *et al.* Mutant huntingtin impairs post-Golgi trafficking to lysozomes by delocalizing optineurin/Rab8 complex from the Golgi apparatus. *Mol. Biol. Cell* 20, 1478–1492 (2009).
22. Takarada, T. *et al.* A protein–protein interaction of stress-responsive myosin VI endowed to inhibit neural progenitor self-replication with RNA binding protein, TLS, in murine hippocampus. *J. Neurochem.* 110, 1457–1468 (2009).
23. Yoshimura, A. *et al.* Myosin-Va facilitates the accumulation of mRNA/protein complex in dendritic spines. *Curr. Biol.* 16, 2345–2351 (2006).

**Supplementary Information** is linked to the online version of the paper at www.nature.com/nature.

**Acknowledgements** This work was supported in part by grants-in-aid from the Ministry of Education, Science, and Culture of Japan, by a grant from the Smoking Research Foundation to H. Kawakami, and by the Japan Science and Technology Agency, Core Research of Evolutional Science & Technology to T.T. We thank E. Nakajima for technical support, K. Nakayama, H.W. Shin, M. Omi and

H. Nakamura for conducting some of the experiments, and T. Miki and K. Noda for providing some DNA samples and clinical information. This paper is dedicated to the patients and families who contributed to this project.

**Author Contributions** H. Kawakami designed and supervised the study. H.Mo. and K.H. extracted candidate genes. H.Ma. and M.K. performed sequencing analysis. H.Ma., H.Mo., Y.W., T.T., S.M., H. Kawakami and H.S. conducted molecular biological analysis. H.I., Y.K., H. Ku., H. Kato, K.O. and A.H. performed pathological analysis and provided pathological samples. Y.I., H.N., R.K., O.K., N.M., K.A., A.K., T.H, T.K., M.A., N.S. and K.K. collected clinical information and samples. H. Kawakami, H.Ma., H.I. and K.H. wrote the paper.

**Author Information** Reprints and permissions information is available at www.nature.com/reprints. The authors declare no competing financial interests. Correspondence and requests for materials should be addressed to H. Kawakami (hkawakam@hiroshima-u.ac.jp).

## METHODS

**Ethical considerations.** The study was approved by the institutional review boards of the participating institutions. All examinations were performed after having obtained informed consent from all subjects or their families.

**Subjects.** Neurologists performed the clinical diagnosis. The mean age at onset of subjects with ALS was 59.9 years (range 10–85 years, including 14 cases confirmed by autopsy). The possibility of mutation of SOD1 was excluded.

**Screening for the mutation of *OPTN*.** A list of PCR primer pairs used to amplify individual *OPTN* in the regulatory regions (~1,000 bases upstream from transcription start sites), non-coding exons, coding exons and the surrounding sequences (50–100 bases) of the exons or intron 4 and 5 is provided in Supplementary Table 4. Deletion of Exon 5 was checked by using exon 4 forward and intron 5 reverse primer pairs. Direct sequence of the joining part was performed by using intron 4-2 forward primer or intron 5-6 reverse primer. Screening for the c.1502C>T mutation was performed by analysing restriction-fragment length polymorphism or direct sequencing on 781 healthy control subjects (mean age 62.3 years; range 30–100 years). Exon 12 was amplified and then restricted with MseI, and thereafter the products were electrophoresed in 2% agarose gel. The wild type was digested into 204-, 106-, 14- and 12-bp fragments, and the mutant type (204 bp) into 169 + 35-bp fragments. The c.1743A>G mutation was determined by direct sequencing. In the Affymetrix Mapping 500K, there were 11 SNPs in the *OPTN* gene. However, there are no SNP markers between exon 2 and exon 12 of *OPTN*, and additional quantitative PCR analysis of all exons of the *OPTN* gene was performed.

**Luciferase assay.** We investigated the activity of NF-κB by using the luciferase assay. Four types of complementary DNA (cDNA) from OPTN were inserted into separate pDNR (Clontech). These were wild (IMAGE clone 3831267), Q398X (recessive), E478G (dominant) and E50K (which causes glaucoma) types. pDNR vector was used as mock. NSC-34 cells were co-transfected with NF-κB reporter ($(Igk)_3$ conaluc plasmid) (a gift from S. Yamaoka) and pDNR-OPTN by using Lipofectamine 2000 (Invitrogen). Luciferase activity was measured 5 h after either PBS or TNF-α (10 ng ml$^{-1}$, R&D) stimulation by using a Dual-Luciferase Reporter Assay System (Promega). Consistent results were obtained by conducting three independent experiments.

**Localization of OPTN.** We investigated the localization of OPTN by using a 3×Flag tag. This was inserted into pcDNA3 (Invitrogen), and three types of OPTN cDNA (wild, E478G, E50K) were inserted after the 3×Flag tag. These plasmids were used to transfect NSC-34 cells with the aid of Lipofectamine 2000 (Invitrogen). GM130 (BD Transduction Laboratories) was used as a marker of the Golgi apparatus.

**Immunofluorescence microscopy.** Cells were grown on glass-bottomed glass dishes (Matsunami) coated with poly-L-lysine and laminin (Sigma Aldrich) and transfected by Lipofectamine 2000 (Invitrogen) according to the manufacturer's protocol; 24–48 h after transfection, the cells were fixed, blocked with normal serum and incubated with primary antibody at 4 °C overnight. Confocal images were acquired with an Olympus FV300 by using a ×100 oil immersion lens with a sequential-acquisition setting at a resolution of 512 pixels × 512 pixels with threefold magnification. Each cellular picture was generated by combining multiple optical images (10–15 slices, *z*-spacing of 0.2 μm) spanning 2–3 μm along the *z*-axis. Subcellular localization of Flag-tagged optineurin was verified by at least three independent experiments. More than 100 cells were photographed for each optineurin construct. The following antibodies were used: mouse monoclonal anti-GM130 (BD Transduction Laboratories, 1:1,000) and affinity-purified rabbit polyclonal anti-Flag (Sigma, 1:1,000).

**Western blotting.** We investigated the expression of OPTN by western blotting. Cell lysates were prepared from Epstein-Barr-virus immortalized B lymphocytes from subject 3, her brother and mother, and subject 4 by using standard protocols. Polyclonal antibodies recognizing the carboxy (C)-terminal part of OPTN (Cayman Chemical) and anti-rabbit IgG-HRP antibody (R&D Systems) were used. For the internal control, we used glyceraldehyde-3-phosphate dehydrogenase polyclonal antibody (IMGENEX).

**Quantitative PCR with reverse transcription.** Quantitative PCR with reverse transcription was performed by using THUNDERBIRD SYBR qPCR Mix (TOYOBO) and ABI 7900HT Fast Real Time PCR system (Applied Biosystems). Epstein-Barr-virus immortalized B lymphocytes were treated with cycloheximide (Sigma, 100 μg ml$^{-1}$) for 2 h before RNA extraction.

**Immunohistochemistry of mouse nervous tissue.** Several antibodies were tested for their use in detecting mouse OPTN in tissue sections (data not shown). Among them, rabbit polyclonal antibodies raised against various peptides of human/mouse OPTN origin gave consistent and reasonable results. One such antibody was OPTN-C raised against the C-terminal part of OPTN, which is identical between human and mouse (amino acids 575–591; Cayman Chemical). Immunohistochemistry was performed on adult DBA/2 mouse. Mice were transcardially fixed with 4% paraformaldehyde in PBS, post-fixed in the same fixative overnight, and then dehydrated in 30% sucrose in PBS overnight. Frozen sections were obtained by using a cryostat and mounted onto 3-triethoxysilylpropylamine (TESPA)-coated glass slides. After air-drying, the slides were washed in PBS and blocked for 2 h at room temperature in 5% BSA/0.3% Triton X-100 containing PBS. The sections were then incubated overnight at 4 °C with primary antibodies against OPTN diluted in 1% BSA/1% normal goat serum/0.3% Triton X-100/PBS. After several washes in PBS, Alexa-594-conjugated secondary antibody (Invitrogen) in PBS was applied. Pictures were taken with a camera attached to a fluorescence microscope (BIOREVO BZ-9000; Keyence).

**Histochemistry.** Post-mortem material from one of the OPTN mutant cases (subject 5) was available. Sections (6 μm) of formalin-fixed, paraffin-embedded spinal cord were examined with Klüver–Barrera and haematoxylin and eosin staining. Some sections stained with haematoxylin and eosin were photographed, decolourized and immunostained with OPTN-C (mouse monoclonal, 1: 50,000) or OPTN-1 (rabbit polyclonal, Cayman Chemical, 1:400). In addition, lumbar spinal cord tissue was obtained from clinically and neuropathologically proven cases of SALS (seven cases) and familial ALS with the A4V *SOD1* mutation (FALS, three cases). Six age-matched normal individuals served as controls. After confirmation of complete removal of the OPTN antibody, we immunostained the same sections with the anti-ubiquitin antibodies (mouse monoclonal, Santa Cruz Biotechnology, 1:400; rabbit polyclonal, Sigma, 1:600), anti-TDP-43 antibodies (mouse monoclonal, Abnova, 1:1,000; rabbit polyclonal, Proteintech Group, 1:4,000) or anti-SOD1 antibodies (mouse monoclonal, Lab Vision Corporation, 1:50; rabbit polyclonal, Stressgen Biotechnologies, 1:2,000).

# Author Queries

Journal: **Nature**
Paper: **nature08971**
Title: **Mutations of optineurin in amyotrophic lateral sclerosis**

| Query Reference | Query |
|---|---|
| 1 | AUTHOR: When you receive the PDF proofs, please check that the display items are as follows (doi:10.1038/nature08971): Figs 0 (black & white); 1–3 (colour); Tables: None; Boxes: None. Please check all figures very carefully as they have been re-labelled, re-sized and adjusted to Nature's style. Please ensure that any error bars in the figures are defined in the figure legends. Please check all author names, affiliations and Acknowledgements carefully to ensure that they are correct. |
| 2 | Proofreader: Please update/confirm the tentative publication date |
| 3 | Author: definitions of JST and CREST OK? Else, please spell out. |

**For Nature office use only:**

| | | | | | |
|---|---|---|---|---|---|
| Layout | ☐ | Figures/Tables/Boxes | ☐ | References | ☐ |
| DOI | ☐ | Error bars | ☐ | Supp info (if applicable) | ☐ |
| Title | ☐ | Colour | ☐ | Acknowledgements | ☐ |
| Authors | ☐ | Text | ☐ | Author contribs (if applicable) | ☐ |
| Addresses | ☐ | Methods (if applicable) | ☐ | COI | ☐ |
| First para | ☐ | Received/Accepted | ☐ | Correspondence | ☐ |
| Display items | ☐ | AOP (if applicable) | ☐ | Author corrx | ☐ |

Journal of Neuroscience Research

Journal of Neuroscience Research 88:1804–1811 (2010)

# Induction of Parkinsonism-Related Proteins in the Spinal Motor Neurons of Transgenic Mouse Carrying a Mutant SOD1 Gene

**Nobutoshi Morimoto,[1]* Makiko Nagai,[1] Kazunori Miyazaki,[1] Yasuyuki Ohta,[1] Tomoko Kurata,[1] Yasushi Takehisa,[1] Yoshio Ikeda,[1] Tohru Matsuura,[1] Masato Asanuma,[2] and Koji Abe[1]**

[1]Department of Neurology, Graduate School of Medicine, Dentistry and Pharmaceutical Science, Okayama University, Okayama, Japan

[2]Department of Brain Science, Graduate School of Medicine, Dentistry and Pharmaceutical Science, Okayama University, Okayama, Japan

Amyotrophic lateral sclerosis is a progressive and fatal disease caused by selective death of motor neurons, and a number of these patients carry mutations in the superoxide dismutase 1 (SOD1) gene involved in ameliorating oxidative stress. Recent studies indicate that oxidative stress and disruption of mitochondrial homeostasis is a common mechanism for motor neuron degeneration in amyotrophic lateral sclerosis and the loss of midbrain dopamine neurons in Parkinson's disease. Therefore, the present study investigated the presence and alterations of familial Parkinson's disease-related proteins, PINK1 and DJ-1, in spinal motor neurons of G93ASOD1 transgenic mouse model of amyotrophic lateral sclerosis. Following onset of disease, PINK1 and DJ-1 protein expression increased in the spinal motor neurons. The activated form of p53 also increased and translocated to the nuclei of spinal motor neurons, followed by increased expression of p53-activated gene 608 (PAG608). This is the first report demonstrating that increased expression of PAG608 correlates with activation of phosphorylated p53 in spinal motor neurons of an amyotrophic lateral sclerosis model. These results provide further evidence of the profound correlations between spinal motor neurons of amyotrophic lateral sclerosis and parkinsonism-related proteins. 

**Key words:** amyotrophic lateral sclerosis; Parkinson's disease; PINK1; DJ-1; PAG608

Amyotrophic lateral sclerosis (ALS), a progressive and fatal disease caused by the selective death of motor neurons, is due to a genetically inherited form of the disease known as familial ALS (FALS) in approximately 5–10% of ALS patients. Previous reports have shown that approximately 20% of FALS patients carry mutations in the superoxide dismutase 1 (SOD1) gene (Aoki et al., 1993; Rosen et al., 1993). Transgenic mice expressing mutant forms of the SOD1 gene have demonstrated how mutations in the SOD1 gene cause motor neuron death. The process is considered to be a toxic gain-of-function, rather than loss of normal SOD1 function (Bowling et al., 1995). Although the primary pathogenetic mechanisms remain poorly understood, the appearance of vacuoles due to degenerated mitochondria, as well as selective loss of spinal motor neurons, is a hallmark of mutant SOD1 transgenic (Tg) mice (Wong et al., 1995; Bendotti et al., 2001; Sasaki et al., 2009). Moreover, our previous studies showed oxidative damage to cytosolic protein (Abe et al., 1995) and mitochondrial DNA in spinal motor neurons of ALS model mice at early disease stages (Warita et al., 2001; Murakami et al., 2007). Therefore, mitochondrial oxidative stress has been suggested as an ALS pathogenic mechanism.

In contrast, Parkinson's disease (PD) is an age-related, neurodegenerative disease. Although the causes for sporadic cases remain unknown, mitochondrial or oxidative toxins, such as 1-methyl-4-phenylpyridinium, 6-hydroxydopamine (6-OHDA), and rotenone reproduce disease features in animal and cell culture models (Bove et al., 2005). Increased oxidative stress has been

Contract grant sponsors: Ministry of Education, Science, Culture and Sports of Japan; Contract grant sponsor: Ministry of Health and Welfare of Japan (to Y.I., T.I., and I.N.); Contract grant sponsor: Grant-in-Aid for Scientific Research; Contract grant number: (B) 21390267.

*Correspondence to: Nobutoshi Morimoto, Department of Neurology, Graduate School of Medicine, Dentistry and Pharmaceutical Science, Okayama University, 2-5-1 Shikata-cho, Okayama 700-8558, Japan. E-mail: morinobu@cc.okayama-u.ac.jp

Received 31 July 2009; Revised 23 October 2009; Accepted 1 November 2009

**Published online 1 February 2010 in Wiley InterScience (www.interscience.wiley.com). DOI: 10.1002/jnr.22341**